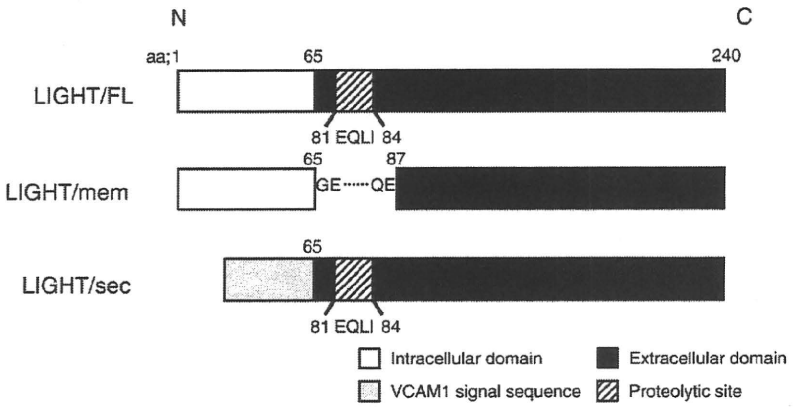

Fig. 1. Schematic representation of LIGHT/FL, LIGHT/mem, and LIGHT/sec. LIGHT/mem; amino acids 66 to 86, including the proteolytic site, were deleted from full-length LIGHT to ensure stable surface expression by tumor cells. LIGHT/sec; extracellular domain of LIGHT, amino acids 66 to 240, was fused to the C-terminus of the VCAM1 signal peptide.

superfamily, for example Fas ligand (FasL) and TNF-α [12,13]. Gregory et al. reported a marked difference in the anti-tumor effect between secreted FasL and membrane-anchored FasL in tumor cells constitutively expressing these proteins [16]. Similar to FasL, native LIGHT also exists as a membrane-anchored form and is proteolytically cleaved from the membrane by matrix metalloproteinases (MMP) to produce the mature, secreted, 25-kDa form [6,17,18]. Differences in the function and anti-tumor activity of native full-length LIGHT (LIGHT/FL), stably membrane-anchored LIGHT (LIGHT/mem), and fully secreted LIGHT (LIGHT/sec), remain unknown, but understanding these differences is necessary to identify the optimal form of LIGHT for cancer gene therapy.

Here, we investigated the differences in anti-tumor activity between native, secreted and membrane-anchored LIGHT. First, we constructed Arg-Gly-Asp (RGD) fiber-mutant adenovirus (Ad) vectors (AdRGD), which efficiently transfer foreign genes into target cells, including tumor cells, to express LIGHT/FL, LIGHT/mem, or LIGHT/sec. Then, we compared the anti-tumor effects of the different forms of LIGHT *in vivo* by intratumoral injection of each AdRGD.

2. Materials and methods

2.1. Cells and animals

HT29.14S cells, which are clones of the HT29 colon adenocarcinoma cell line, were kindly provided by Dr. CF Ware (La Jolla Institute for Allergy and Immunology, CA) and cultured in DMEM supplemented with 10% FBS and antibiotics. Murine colon carcinoma CT26 cells were kindly provided by Dr. NP Restifo (National Cancer Institute, Bethesda, MD), cultured in RPMI 1640 medium supplemented with 10% FBS and antibiotics. Murine melanoma B16BL6 cells were purchased from the JCRB cell bank (Tokyo, Japan) and cultured in MEM supplemented with 7.5% FBS and antibiotics. Female BALB/c mice and C57BL/6 mice were purchased from Nippon SLC (Kyoto, Japan) and used at 6 to 8 weeks of age. All of the animal experimental procedures in this study were performed in accordance with the Osaka University guidelines for the welfare of animals.

2.2. Construction of Ads

Human LIGHT cDNA was kindly provided by Dr. K Tamada (University of Maryland, Baltimore, MD). We used full-length human LIGHT sequence as a template to generate DNA fragments by PCR: fragment-LIGHT/FL, fragment-LIGHT/mem, and fragment-LIGHT/sec. For fragment-LIGHT/FL, sense primer 5′-CGTCTAGAATGGAGGAGAGTGTCGTACGG CCCTC-3′ and antisense primer 5′-ATGCGGCCGC TCATCACACC ATGAAAGCCC CGAAG-3′ were used; for fragment-LIGHT/mem, sense primer 5′-CTCCCTGCAGCT GCACTGGCGTCTACGAAGGTCTCACGAGGTCAACCCAG-3′ and the antisense primer described above were used; for fragment-LIGHT/sec, sense primer 5′-CGTCTAGAATGCCTGGGAAGATGGTCGTGATCCTTGGAGCCT-CAAATATACTTTGGATAATGTTTGCAGCTTCTCAAGCTGGAGAGATGGT-CACCCGCCTGCC-3′ and the antisense primer described above were used. The resultant products were cloned into pHM-CMV5. Then AdRGD-LIGHTs that carried the various forms of the human LIGHT gene were constructed by an improved *in vitro* ligation method [19,20]. Each Ad was generated by established methods [19]. Luciferase-expressing AdRGD (AdRGD-Luc) was previously constructed [21]. The virus particles and biological titer (infectious unit; IFU) were determined by a spectrophotometrical method and by using an Adeno-X Rapid Titer protocol (Clontech Laboratories, Mountain View, CA, USA), respectively [22]. The particle-to-biological titer ratio was between 10 and 40 for each Ad used in this study.

2.3. Evaluation of production levels of LIGHT from transduced cells in vitro

HT29.14S and B16BL6 cells were transduced with each Ad for 2 h at 500 IFU/cell. The cells were washed and cultured for another 22 h in media containing 10% FBS. The supernatants were collected, and the level of LIGHT for each Ad was measured with the Human LIGHT Enzyme Immunosorbent Assay Kit (R&D Systems, Minneapolis, MN). The expression level of LIGHT on the cell surface was assessed with the anti-human LIGHT/TNFSF14 monoclonal antibody (R&D systems) and a FITC-conjugated rat anti-mouse Igκ light chain monoclonal antibody (BD Pharmingen, San Diego, CA) by flow cytometry on a FACSCalibur flow cytometer.

2.4. Cytotoxicity assay

HT29.14S cells (5000 cells/well) were incubated for 12 h at 37 °C. Then cells were transduced with AdRGDs at 10, 100, or 500 IFU/cell in the presence of 10 units/mL human IFN-γ. After 56 h, cell viability was assessed by the WST-8 assay according to the manufacturer's instructions. The OD450-650 was measured with a multiwell spectrophotometer (Spectra Max M5Y, Molecular Devices, Inc.).

2.5. Animal studies

C57BL/6 mice or BALB/c mice were intradermally inoculated with 2×10^5 cells (B16BL6) or 5×10^5 cells (CT26), respectively, into the flank. Seven days later, established tumors with diameters of 5–7 mm were treated with each Ad at 5×10^8 (B16BL6) or 7×10^7 (CT26) IFU in 50 μL PBS, respectively. Tumor size was measured with calipers 3 times a week, and tumor volume was calculated using the following

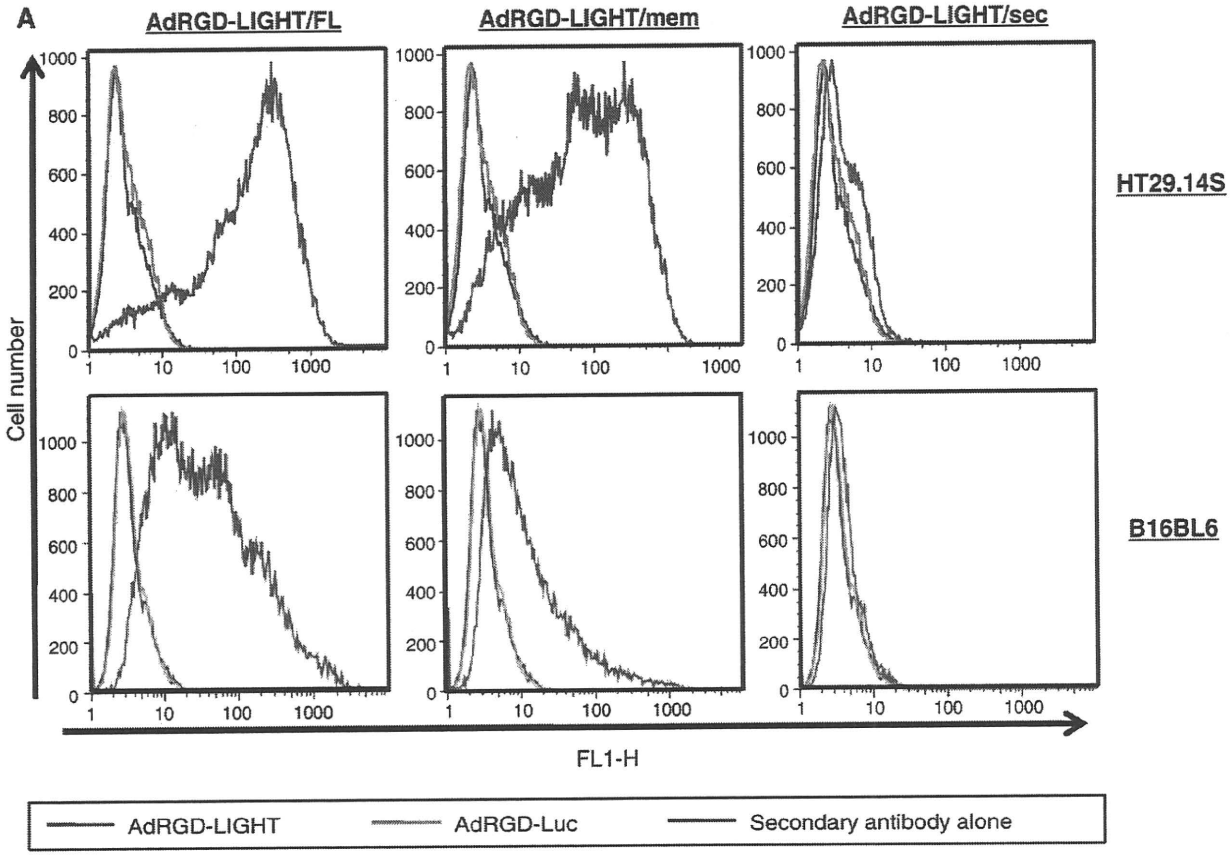
A
AdRGD-LIGHT/FL
AdRGD-LIGHT/mem
AdRGD-LIGHT/sec
HT29.14S
B16BL6
Cell number
FL1-H
AdRGD-LIGHT
AdRGD-Luc
Secondary antibody alone

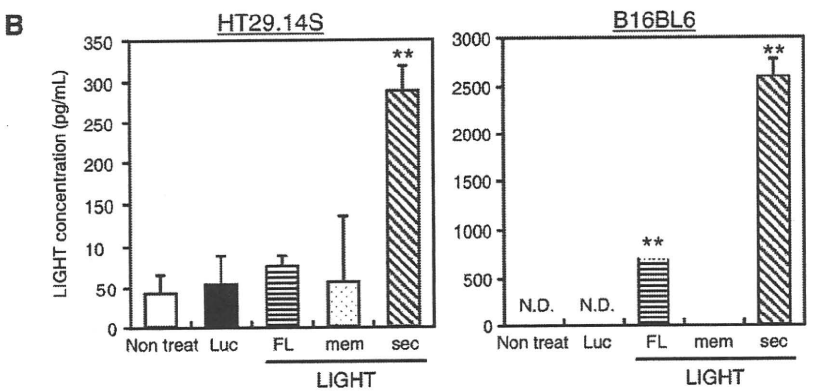
B
HT29.14S
B16BL6
LIGHT concentration (pg/mL)
N.D.
Non treat
Luc
FL
mem
sec
LIGHT

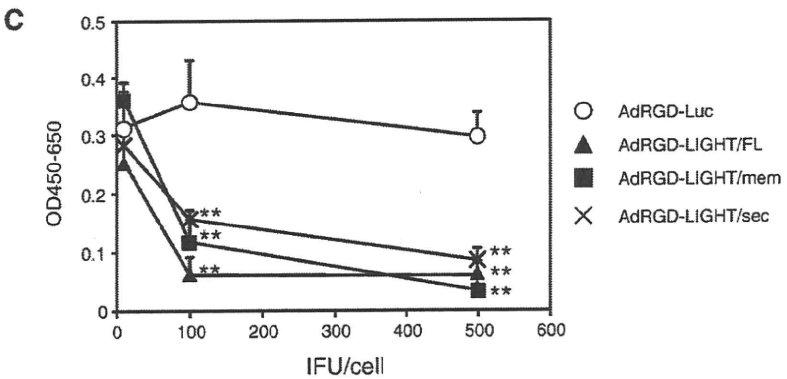
C
OD450-650
IFU/cell
AdRGD-Luc
AdRGD-LIGHT/FL
AdRGD-LIGHT/mem
AdRGD-LIGHT/sec

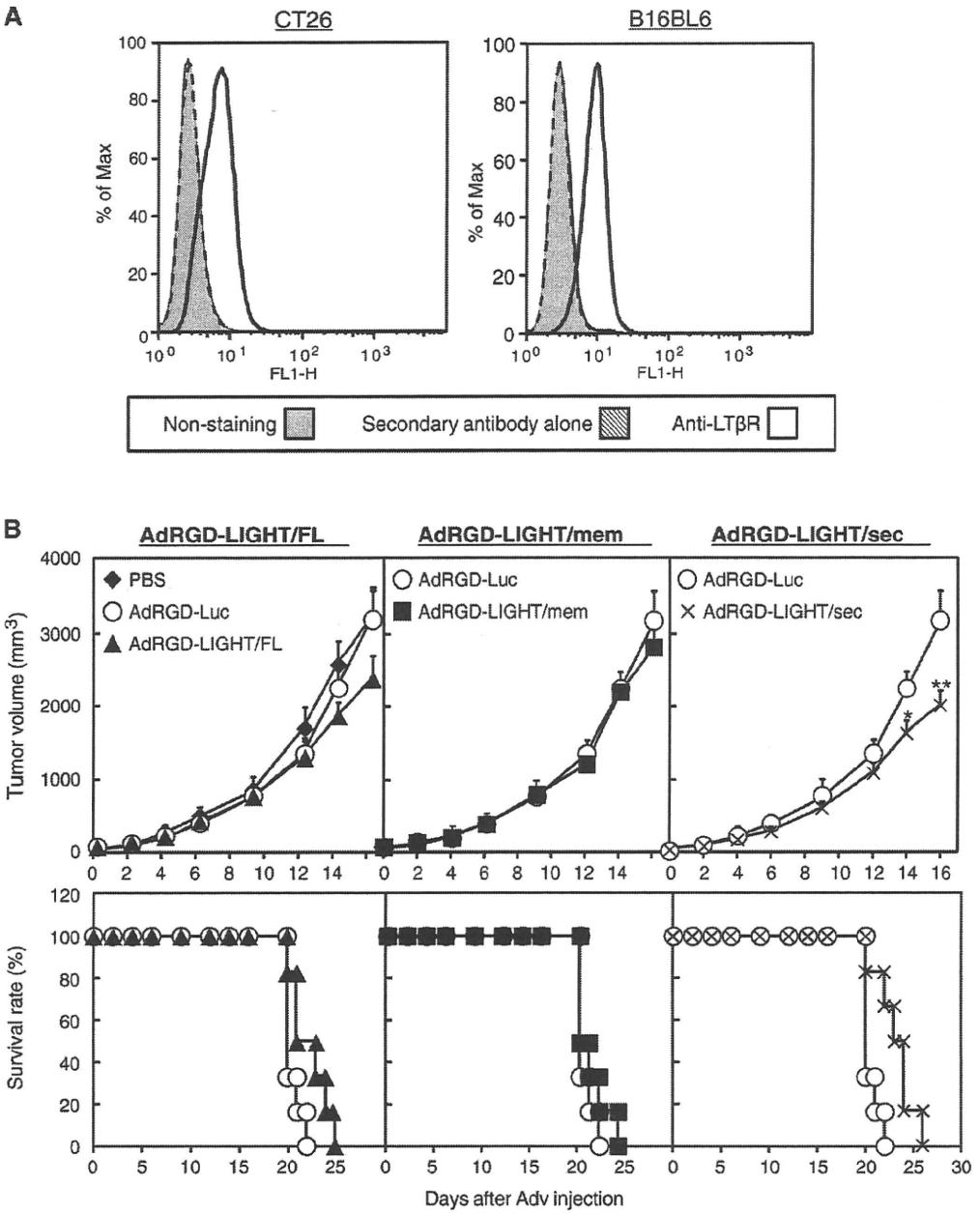

Fig. 3. Therapeutic effect of intratumorally injected AdRGD-LIGHTs. (A) LTβR expression in CT26 and B16BL6 cells. LTβR expression on the cell surface of CT26 and B16BL6 cells was determined by flow cytometry analysis using the anti-LTβR antibody. The open curve shows staining with the anti-mouse LTβR antibody. The filled and slashed curves show non-staining and the secondary antibody only control. (B) B16BL6 cells (2×10^5 cells/mouse) or (C) CT26 cells (5×10^5 cells/mouse) were intradermally inoculated into C57BL/6 or BALB/c mice, respectively. Seven days later, the tumors were treated with the AdRGD-LIGHTs. The tumor volume and prolonged survival time of tumor-bearing mice were monitored. Data were calculated according to the formula described in Section 2, and each point represents the mean ± SEM for six mice. (* $P<0.05$ and ** $P<0.01$ compared with AdRGD-Luc by the Student's *t*-test.).

formula: (tumor volume; mm^3) = (major axis; mm) × (minor axis; $mm)^2\times0.5$. Mice bearing tumors with a major axis greater than 25 mm were euthanized. All animal experiments were carried out in accordance with protocols approved by the Animal Care and Use Committee of the Graduate School of Pharmaceutical Sciences, Osaka University, Japan.

Fig. 2. Confirmation of the form and biological activity of LIGHT. (A) Flow cytometric analysis of LIGHT expression. HT29.14S and B16BL6 cells were transduced with AdRGD-LIGHTs at the dose of 500 IFU/cell. The expression of LIGHT on the cell surface was detected by flow cytometric analysis. The blue curve shows staining with the anti-human LIGHT antibody. (B) Quantification of the secreted soluble form of LIGHT by ELISA. HT29.14S and B16BL6 cells were transduced with AdRGD-LIGHTs at the dose of 500 IFU/cell. LIGHT concentration in the culture supernatant was measured by ELISA. Each point represents the mean ± SD. (** $P<0.01$ versus value for AdRGD-Luc by ANOVA.) (C) Confirmation of biological activity of LIGHT expressed by each AdRGD. HT29.14S cells were transduced with AdRGD-LIGHTs in the presence of 10 units/mL of human IFN-γ. These transduced cells were incubated for 56 h. Cytotoxicity was evaluated by the WST-8 assay. Each point represents the mean ± SD. (** $P<0.01$ versus value for AdRGD-Luc by ANOVA.).

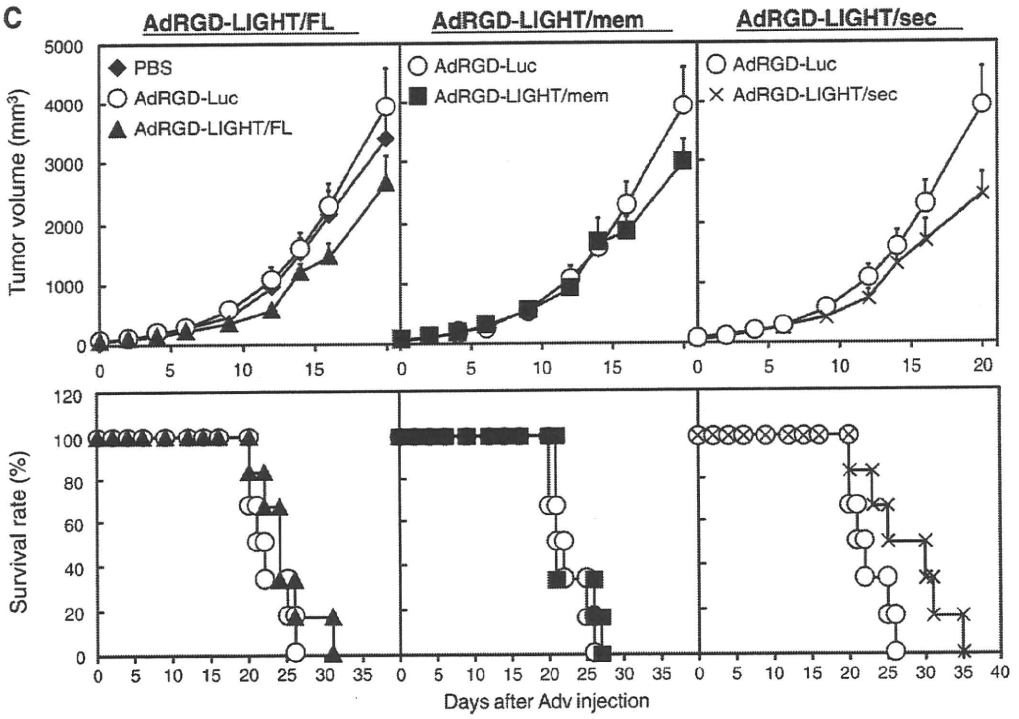

Fig. 3 (*continued*).

2.6. Detection of CD4+ and CD8+ T cells in tumors

BALB/c mice were intradermally inoculated with 5×10^5 CT26 cells into the flank. Seven days later, established tumors with diameters of 5–7 mm were treated with each Ad at 7×10^7 IFU. Eighteen days after intratumoral injection with Ads, CT26 tumors were removed, embedded in OCT compound (Sakura Finetechnical, Tokyo, Japan), and frozen in liquid nitrogen. Frozen sections (7 μm thick) were fixed in 4% paraformaldehyde at 4 °C for 10 min and treated with a primary anti-mouse CD4 or anti-mouse CD8 antibody (BD Pharmingen) at room temperature for 2 h. After washes, the sections were stained with the secondary antibody conjugated with Alexa Fluor 594 Anti-Rat IgG (Molecular Probes) at room temperature for 2 h. Then, the frozen sections were mounted with Prolong Gold with DAPI (Invitrogen, Carlsbad, CA) for nuclear staining, and then photographed with a fluorescence microscope (BZ-8000; Keyence Corporation, Osaka, Japan). Quantification of CD4+ and CD8+ cells in the frozen sections was performed by counting the number of cells in four random high-power fields.

2.7. Statistical analysis

All results are expressed as means ± SEM or SD. Differences were compared by using the Student's *t*-test or Scheffe's method after analysis of variance (ANOVA).

3. Results

3.1. Construction of Ad vectors encoding various forms of LIGHT

We used the AdRGD system, which exhibits α_v-integrin tropism due to an RGD peptide inserted into the HI loop of the fiber knob, to achieve high levels of LIGHT gene expression. This vector system has superior gene transduction efficiency of cancer cells *in vitro* and *in vivo* compared with the conventional Ad vectors [21,23]. We constructed AdRGD encoding LIGHT/FL, which is sensitive to ectodomain shedding creating both secreted and membrane-anchored forms of LIGHT. We also constructed AdRGD encoding only LIGHT/mem, which lacks amino acids from Gly66 to Glu86, including the key proteolytic site (amino acid Glu81-Ile84), and AdRGD encoding only LIGHT/sec, which consists of an extracellular domain of LIGHT composed of amino acids Gly66 to Val240 linked to a signal peptide from VCAM1 to direct secretion (Fig. 1).

3.2. Confirmation of biological activity of various forms of LIGHT

To confirm that each AdRGD-LIGHT constructed here expressed the LIGHT protein in the intended form, we examined the expression patterns of LIGHT on the surface or in the culture supernatant of cells transduced with each AdRGD. First, we analyzed the expression of the LIGHT protein on the surface of HT29.14S or B16BL6 cells by flow cytometry. We detected LIGHT on the surface of HT29.14S and B16BL6 cells transduced with AdRGD-LIGHT/FL and AdRGD-LIGHT/mem, but not on the surface of those transduced with AdRGD-LIGHT/sec or the AdRGD-Luc control (Fig. 2A). Then, to confirm the expression of the secreted form of LIGHT, we quantified the levels of the LIGHT protein in the culture supernatant of transduced HT29.14S and B16BL6 cells by ELISA. We found that for HT29.14S and B16BL6 cells, AdRGD-LIGHT/sec secreted higher levels of LIGHT than AdRGD-LIGHT/FL or AdRGD-LIGHT/mem (Fig. 2B). For B16BL6 cells transduced with AdRGD-LIGHT/FL, we also detected secreted LIGHT in the culture supernatant. This is probably the result of cleavage of full-length LIGHT expressed on the cellular surface by MMP produced by B16BL6 cells. On the other hand, we did not detect LIGHT in the culture supernatant of cells transduced with AdRGD-LIGHT/mem or AdRGD-Luc control. Taken together, these results show that each AdRGD-LIGHT expressed the intended form of LIGHT protein, at least when transfected into B16BL6 cells. By comparison, we could not detect LIGHT in the culture supernatant of HT29.14S cells transfected with AdRGD-LIGHT/FL. We consider that this is probably because HT29.14S cells do not express MMPs.

Next, to examine whether the LIGHT proteins expressed by each AdRGD-LIGHT were biologically active, we transduced HT29.14S cells, which are sensitive to the proapoptotic effect of LIGHT, with the AdRGD-

LIGHTs in the presence of 10 units/mL of human IFN-γ (Fig. 2C) [5,24]. We found that the viability of HT29.14S cells transduced with each AdRGD-LIGHT was significantly lower than the viability of cells transduced with the control vector AdRGD-Luc and was dependent upon vector dose. These results indicate that AdRGD-LIGHTs constructed here express LIGHT with sustained activity.

3.3. Therapeutic effect of intratumorally injected AdRGD-LIGHTs

To assess the therapeutic potential of the AdRGD-LIGHTs, we evaluated the anti-tumor effect of a single intratumoral injection of each AdRGD-LIGHT in mice bearing established B16BL6 and CT26 tumors [25,26]. The expression of LTβR by B16BL6 cells and CT26 cells was confirmed by flow cytometric analysis (Fig. 3A). In both Bl6BL6 and CT26 tumors, tumor growth in mice treated with AdRGD-Luc was comparable to that of PBS-treated mice (Fig. 3B, C). In the B16BL6 tumor model, AdRGD-LIGHT/FL and AdRGD-LIGHT/sec showed tumor-suppressing effects, whereas AdRGD-LIGHT/mem did not (Fig. 3B). Furthermore, AdRGD-LIGHT/sec had a stronger tumor-suppressing effect than AdRGD-LIGHT/FL. In the CT26 tumor model, AdRGD-LIGHT/sec provided the strongest tumor-suppressing effect of all the AdRGD-LIGHTs and tended to prolong the survival more than the AdRGD-Luc

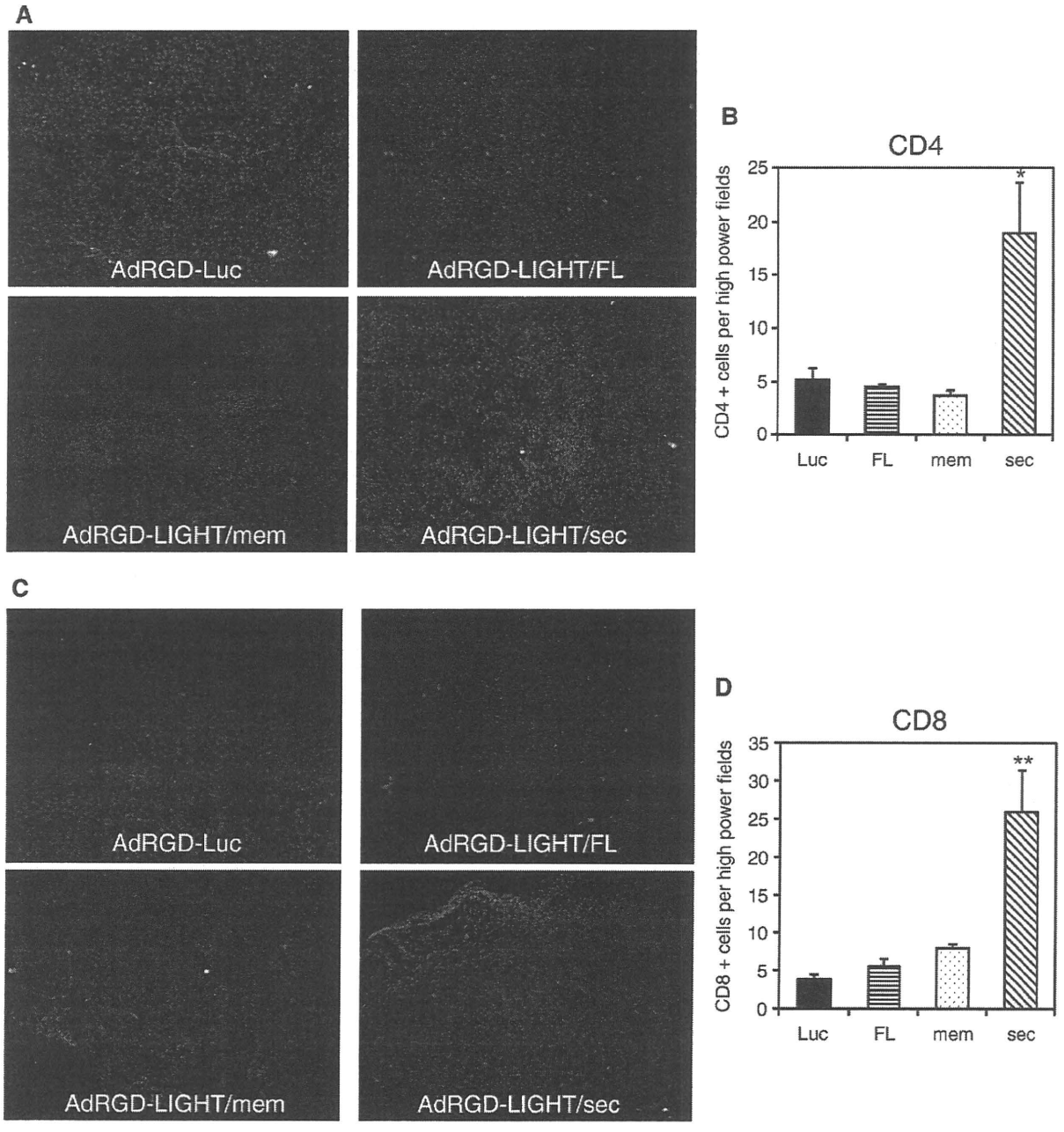

Fig. 4. Histological analysis of tumors administered each AdRGD-LIGHT. CT26 cells (5×10^5 cells/mouse) were intradermally inoculated into BALB/c mice. Seven days later, the tumors were intratumorally treated with each AdRGD-LIGHT. Tumor tissues were collected 18 days after injection and were then embedded in OCT compound and frozen. (A) Frozen sections of tumor tissues were fixed and stained with an anti-mouse CD4 antibody together with an Alexa Fluor 594-conjugated secondary antibody. (B) Quantification of CD4+ cells. (C) Tumors were similarly stained with an anti-mouse CD8 antibody together with an Alexa Fluor 594-conjugated secondary antibody. (D) Quantification of CD8+ cells. Each bar represents the mean ± SEM of the number of CD4+ or CD8+ cells in four random high-power fields (* $P<0.05$ and ** $P<0.01$ versus value for AdRGD-Luc by ANOVA).

control, but this difference was not significant (Fig. 3C). These data indicate that the rank order of the anti-tumor effect of these 3 forms of LIGHT was LIGHT/sec > LIGHT/FL > LIGHT/mem. In addition, we confirmed that mice treated with the AdRGD-LIGHTs did not lose body weight (data not shown). These results suggest that AdRGD-LIGHT/sec efficiently suppresses tumor growth without severe side effects.

3.4. The mechanism of anti-tumor effects of AdRGD-LIGHT/sec

To investigate the mechanism underlying the anti-tumor effects of AdRGD-LIGHT/sec, we assessed the infiltration of immune cells into the tumor mass following intratumoral administration of each AdRGD-LIGHT (Fig. 4). At 18 days after injection, intradermal tumor nodules were resected from tumor-bearing mice for histological examination. We observed more extensive infiltration of CD4+ (Fig. 4A, B) and CD8+ (Fig. 4C, D) T cells in tumors of mice treated with AdRGD-LIGHT/sec than in those treated with the AdRGD-Luc control. By comparison, there was little or no infiltration of CD4+ and CD8+ cells in tumors of mice treated with AdRGD-LIGHT/FL or LIGHT/mem compared with those treated with the AdRGD-Luc control. These findings suggest that the substantial increase in the number of CD4+ and CD8+ T cells within tumors induced by AdRGD-LIGHT/sec might activate tumor-specific immunity in mice.

4. Discussion

LIGHT is a promising candidate for cancer therapy [10,27,28]. However, the difference in anti-tumor activity between membrane-anchored and secreted LIGHT has not been well defined. Here, we compared the potency of the anti-tumor effect of different forms of LIGHT to identify the optimal form for cancer gene therapy.

It has been reported that, in mouse tumor models, membrane-anchored LIGHT exhibits a potent therapeutic effect against various cancers [6,11]. However, in our therapeutic model, secreted LIGHT exhibited a superior therapeutic effect: a single intratumoral injection of AdRGD-LIGHT/sec gave the most efficient anti-tumor effect of all forms of LIGHT, whereas AdRGD-LIGHT/mem gave negligible tumor suppression. Although the mechanism underlying this phenomenon remains unclear, we confirmed that B16BL6 and CT26 cells were resistant to the proapoptotic effect of LIGHT (data not shown), and therefore in our therapeutic model, the main contributing factor to the tumor-suppressing effect of LIGHT might be the activation of cancer immunity. We hypothesized that secreted LIGHT expressed by AdRGD-LIGHT/sec might be efficiently distributed throughout the tumor mass and could induce cancer immunity over a broad area of the tumor, whereas membrane-anchored LIGHT might be restricted to a limited area near the AdRGD vector injection site. This notion was confirmed by our finding that AdRGD-LIGHT/sec efficiently induced infiltration of CD4+ and CD8+ T cells in the tumor mass, whereas LIGHT/mem failed to do so (Fig. 4). However, we observed only a slight, not dramatic, therapeutic effect of AdRGD-LIGHT/sec. In this study, we used the human LIGHT, which was shown by Shaikh et al. to bind to the mouse LTβR and mouse HVEM with an affinity nearly 10-fold lower than that of mouse LIGHT [29]. Thus, we speculate that the inadequate susceptibility of CT26 and B16BL6 tumors to AdRGD-LIGHT/sec in our therapeutic model is the result of differences between human and mouse LIGHT.

Successful cancer gene therapy requires treatment of not only the primary tumor but also distant metastases, which are the major cause of mortality from cancer. Yu et al. reported that local delivery of the gene encoding LIGHT/mem into the primary tumor prevents the formation of metastases [11]. They showed that the primary tumor becomes a major site for the production of CTL, which eradicates established metastatic tumors. Here, we showed that treatment by AdRGD-LIGHT/sec induces T-cell activation within the tumor mass. Moreover, Lukashev et al. examined the production of LTβR in human tumor tissues and found that 87% to 96% of colorectal, lung, larynx/pharynx, stomach, and melanoma tumors were positive for LTβR [30]. Thus, we speculate that AdRGD-LIGHT/sec might have the potential to restrain metastasis and recrudescence of tumors.

In this study, we compared the anti-tumor potential of various forms of LIGHT expressed by AdRGD-LIGHTs and showed that secreted LIGHT had the strongest anti-tumor activity in mouse models of aggressive and established tumors. These results suggest that the secreted form of LIGHT might be the optimal form for cancer gene therapy.

Acknowledgements

The authors declare no conflict of interests. This study was supported in part by grants from the Ministry of Health, Labor, and Welfare of Japan; by the Research on Health Sciences focusing on Drug Innovation from the Japan Health Sciences Foundation; and by the Takeda Science Foundation.

References

[1] Mauri DN, Ebner R, Montgomery RI, Kochel KD, Cheung TC, et al. LIGHT, a new member of the TNF superfamily, and lymphotoxin alpha are ligands for herpesvirus entry mediator. Immunity 1998;8:21–30.
[2] Harrop JA, McDonnell PC, Brigham-Burke M, Lyn SD, Minton J, Tan KB, et al. Herpesvirus entry mediator ligand (HVEM-L), a novel ligand for HVEM/TR2, stimulates proliferation of T cells and inhibits HT29 cell growth. J Biol Chem 1998;273:27548–56.
[3] Murphy M, Walter BN, Pike-Nobile L, Fanger NA, Guyre PM, Browning JL, et al. Expression of the lymphotoxin beta receptor on follicular stromal cells in human lymphoid tissues. Cell Death Differ 1998;5:497–505.
[4] Wang J, Foster A, Chin R, Yu P, Sun Y, Wang Y, et al. The complementation of lymphotoxin deficiency with LIGHT, a newly discovered TNF family member, for the restoration of secondary lymphoid structure and function. Eur J Immunol 2002;32:1969–79.
[5] Rooney IA, Butrovich KD, Glass AA, Borboroglu S, Benedict CA, Whitbeck JC, et al. The lymphotoxin-beta receptor is necessary and sufficient for LIGHT-mediated apoptosis of tumor cells. J Biol Chem 2000;275:14307–15.
[6] Yu P, Lee Y, Liu W, Chin RK, Wang J, Wang Y, et al. Priming of naive T cells inside tumors leads to eradication of established tumors. Nat Immunol 2004;5:141–9.
[7] Stopfer P, Mannel DN, Hehlgans T. Lymphotoxin-beta receptor activation by activated T cells induces cytokine release from mouse bone marrow-derived mast cells. J Immunol 2004;172:7459–65.
[8] Tamada K, Shimozaki K, Chapoval AI, Zhai Y, Su J, Chen SF, et al. LIGHT, a TNF-like molecule, costimulates T cell proliferation and is required for dendritic cell-mediated allogeneic T cell response. J Immunol 2000;164:4105–10.
[9] Wang J, Lo JC, Foster A, Yu P, Chen HM, Wang Y, et al. The regulation of T cell homeostasis and autoimmunity by T cell-derived LIGHT. J Clin Invest 2001;108:1771–80.
[10] Fan Z, Yu P, Wang Y, Fu ML, Liu W, Sun Y, et al. NK-cell activation by LIGHT triggers tumor-specific CD8+ T-cell immunity to reject established tumors. Blood 2006;107:1342–51.
[11] Yu P, Lee Y, Wang Y, Liu X, Auh S, Gajewski TF, et al. Targeting the primary tumor to generate CTL for the effective eradication of spontaneous metastases. J Immunol 2007;179:1960–8.
[12] Schneider P, Holler N, Bodmer JL, Hahne M, Frei K, Fontana A, et al. Conversion of membrane-bound Fas(CD95) ligand to its soluble form is associated with downregulation of its proapoptotic activity and loss of liver toxicity. J Exp Med 1998;187:1205–13.
[13] Grell M, Douni E, Wajant H, Lohden M, Clauss M, Maxeiner B, et al. The transmembrane form of tumor necrosis factor is the prime activating ligand of the 80 kDa tumor necrosis factor receptor. Cell 1995;83:793–802.
[14] Esch FS, Keim PS, Beattie EC, Blacher RW, Culwell AR, Oltersdorf T, et al. Cleavage of amyloid beta peptide during constitutive processing of its precursor. Science 1990;248:1122–4.
[15] Subramanian SV, Fitzgerald ML, Bernfield M. Regulated shedding of syndecan-1 and -4 ectodomains by thrombin and growth factor receptor activation. J Biol Chem 1997;272:14713–20.
[16] Gregory MS, Saff RR, Marshak-Rothstein A, Ksander BR. Control of ocular tumor growth and metastatic spread by soluble and membrane Fas ligand. Cancer Res 2007;67:11951–8.
[17] Anand S, Wang P, Yoshimura K, Choi IH, Hilliard A, Chen YH, et al. Essential role of TNF family molecule LIGHT as a cytokine in the pathogenesis of hepatitis. J Clin Invest 2006;116:1045–51.
[18] Morel Y, Schiano de Colella JM, Harrop J, Deen KC, Holmes SD, Wattam TA, et al. Reciprocal expression of the TNF family receptor herpes virus entry mediator and its ligand LIGHT on activated T cells: LIGHT down-regulates its own receptor. J Immunol 2000;165:4397–404.
[19] Mizuguchi H, Kay MA. Efficient construction of a recombinant adenovirus vector by an improved in vitro ligation method. Hum Gene Ther 1998;9:2577–83.

[20] Mizuguchi H, Kay MA. A simple method for constructing E1- and E1/E4-deleted recombinant adenoviral vectors. Hum Gene Ther 1999;10:2013–7.
[21] Mizuguchi H, Hayakawa T. Enhanced antitumor effect and reduced vector dissemination with fiber-modified adenovirus vectors expressing herpes simplex virus thymidine kinase. Cancer Gene Ther 2002;9:236–42.
[22] Maizel Jr JV, White DO, Scharff MD. The polypeptides of adenovirus. I. Evidence for multiple protein components in the virion and a comparison of types 2, 7A, and 12. Virology 1968;36:115–25.
[23] Okada Y, Okada N, Mizuguchi H, Takahashi K, Hayakawa T, Mayumi T, et al. Optimization of antitumor efficacy and safety of in vivo cytokine gene therapy using RGD fiber-mutant adenovirus vector for preexisting murine melanoma. Biochim Biophys Acta 2004;1670:172–80.
[24] Yu KY, Kwon B, Ni J, Zhai Y, Ebner R, Kwon BS, et al. A newly identified member of tumor necrosis factor receptor superfamily (TR6) suppresses LIGHT-mediated apoptosis. J Biol Chem 1999;274:13733–6.
[25] Fearon ER, Itaya T, Hunt B, Vogelstein B, Frost P. Induction in a murine tumor of immunogenic tumor variants by transfection with a foreign gene. Cancer Res 1988;48:2975–80.
[26] Tanaka K, Gorelik E, Watanabe M, Hozumi N, Jay G. Rejection of B16 melanoma induced by expression of a transfected major histocompatibility complex class I gene. Mol Cell Biol 1988;8:1857–61.
[27] Yu P, Fu YX. Targeting tumors with LIGHT to generate metastasis-clearing immunity. Cytokine Growth Factor Rev 2008;19:285–94.
[28] Loeffler M, Le'Negrate G, Krajewska M, Reed JC. Attenuated Salmonella engineered to produce human cytokine LIGHT inhibit tumor growth. Proc Natl Acad Sci U S A 2007;104:12879–83.
[29] Shaikh RB, Santee S, Granger SW, Butrovich K, Cheung T, Kronenberg M, et al. Constitutive expression of LIGHT on T cells leads to lymphocyte activation, inflammation, and tissue destruction. J Immunol 2001;167:6330–7.
[30] Lukashev M, LePage D, Wilson C, Bailly V, Garber E, Lukashin A, et al. Targeting the lymphotoxin-beta receptor with agonist antibodies as a potential cancer therapy. Cancer Res 2006;66:9617–24.

Biomaterials 31 (2010) 3357–3363

Contents lists available at ScienceDirect

Biomaterials

journal homepage: www.elsevier.com/locate/biomaterials

Creation of a LIGHT mutant with the capacity to evade the decoy receptor for cancer therapy

Tomohiro Morishige [a,1], Yasuo Yoshioka [a,b,c,*,1], Hiroshi Inakura [a], Aya Tanabe [a], Xinglei Yao [a], Shin-ichi Tsunoda [b,c], Yasuo Tsutsumi [b,c,d], Yohei Mukai [a], Naoki Okada [a], Shinsaku Nakagawa [a,b,**]

[a] Laboratory of Biotechnology and Therapeutics, Graduate School of Pharmaceutical Sciences, Osaka University, 1-6 Yamadaoka, Suita, Osaka 565-0871, Japan
[b] The Center for Advanced Medical Engineering and Informatics, Osaka University, 1-6 Yamadaoka, Suita, Osaka 565-0871, Japan
[c] Laboratory of Pharmaceutical Proteomics, National Institute of Biomedical Innovation, 7-6-8 Saito-Asagi, Ibaraki, Osaka 567-0085, Japan
[d] Laboratory of Toxicology and Safety Science, Graduate School of Pharmaceutical Sciences, Osaka University, 1-6 Yamadaoka, Suita, Osaka 565-0871, Japan

ARTICLE INFO

Article history:
Received 7 November 2009
Accepted 8 January 2010
Available online 1 February 2010

Keywords:
Affinity
Apoptosis
Bioactivity
Cytokine
Cytotoxicity
Immunomodulation

ABSTRACT

The cytokine LIGHT activates various anti-tumor functions through its two receptors, lymphotoxin β receptor (LTβR) and herpes virus entry mediator (HVEM), and is expected to be a promising candidate for cancer therapy. However, LIGHT is also trapped by decoy receptor 3 (DcR3), which is highly expressed in various tumors. Here, we used phage display technique to create LIGHT mutants that specifically bind LTβR and HVEM, and is not trapped by DcR3 for optimized cancer therapy. We constructed phage library displaying structural variants of LIGHT with randomized amino acid residues. After the affinity panning, we created 6 clones of LIGHT mutants as candidates for DcR3-evading LIGHT. Analysis of binding affinities showed that all candidates had 10-fold lower affinities for DcR3 than wild-type LIGHT, while 5 of the 6 clones had almost the same affinity for LTβR and HVEM. Furthermore, analysis of detailed binding kinetics showed that lower affinity for DcR3 is dependent on their faster off-rate. Further, we showed that the LIGHT mutant had almost the same cytotoxicity via LTβR, and had 62-fold higher DcR3-evading capacity compared to the wild type. Our data provide valuable information for construction of more functional LIGHT mutants that might be powerful tools for cancer therapy.

1. Introduction

The tumor necrosis factor (TNF) superfamily member LIGHT (name derived from homologous to Lymphotoxins, shows Inducible expression, and competes with herpes simplex virus Glycoprotein D for herpes virus entry mediator, a receptor expressed by T lymphocytes) is produced as a glycosylated 29-kDa type-II transmembrane protein by activated T cells, monocytes, granulocytes, and immature dendritic cells [1]. LIGHT binds to two functional cellular receptors, lymphotoxin β receptor (LTβR) and herpes virus entry mediator (HVEM), as well as to a non-functional soluble decoy receptor 3 (DcR3) [2,3]. On engagement with LTβR, LIGHT induces cytotoxicity against some human cancer cells, and promotes cytokine production and the release of the naive T cell-attracting chemokines in stromal cells, thus leading to the increased presence of lymphocytes in tissues [4,5]. In addition, triggering of HVEM signals on T cells by LIGHT co-stimulates T cell proliferation and interferon (IFN)-γ secretion in response to T cell receptor engagement, leading to enhanced T cell immunity [4,6]. Recently, Yu et al. reported that local delivery of the LIGHT gene into primary tumor prevents the formation of metastases by the activation and augmentation of tumor immunity via LTβR and HVEM [5,7]. They showed that the primary tumor becomes a major site for the production of cytotoxic T lymphocyte, leading to the rejection of primary and metastatic tumors in mice [5]. In addition, Lukashev et al. observed that, in clinical human tumor tissues, 87–96% of colorectal, lung, larynx/pharynx, stomach, and melanoma tumors were LTβR-positive [8]. Therefore, we expect that LIGHT might have the potential for superior therapeutic efficiency in immunotherapy for various cancers, and also the potential for marked anti-tumor activity in

* Corresponding author at: The Center for Advanced Medical Engineering and Informatics, Osaka University, 1-6 Yamadaoka, Suita, Osaka 565-0871, Japan. Tel./fax: +81 6 6879 8177.
** Corresponding author at: Laboratory of Biotechnology and Therapeutics, Graduate School of Pharmaceutical Sciences, Osaka University, 1-6 Yamadaoka, Suita, Osaka 565-0871, Japan. Tel.: +81 6 6879 8175; fax: +81 6 6879 8179.
E-mail addresses: yasuo@phs.osaka-u.ac.jp (Y. Yoshioka), nakagawa@phs.osaka-u.ac.jp (S. Nakagawa).
[1] Each author contributed equally to the work.

0142-9612/$ – see front matter © 2010 Elsevier Ltd. All rights reserved.
doi:10.1016/j.biomaterials.2010.01.022

restraining metastasis and recrudescence. In fact, we and others have also demonstrated the usefulness of LIGHT for cancer immunotherapy [7,9–13]. Therefore, LIGHT has recently attracted a great deal of attention as a superior agent for cytokine-based cancer immunotherapy for the eradication of not only local, but also disseminated, metastases.

DcR3, also known as TR6, is a new member of the TNF receptor superfamily [14,15]. DcR3 binds specifically to Fas ligand (FasL), TNF-like molecule 1A (TL1A) and LIGHT. DcR3 lacks a membrane anchor, suggesting its role as a soluble inhibitory factor by binding to its ligands [15–17]. In fact, it has been reported that DcR3 inhibits the cytotoxicity against tumor cells that is induced by Fas–FasL and LTβR–LIGHT signaling, and interferes with T cell co-stimulation mediated by HVEM–LIGHT association [14,18,19]. There is strong evidence that DcR3 is over-expressed in various tumors, including malignant tumors arising from the esophagus, stomach, lung, colon, and rectum [14,20–25]. Wu et al. reported that 56% of tumor patients are serum DcR3-positive, and >70% of patients with gastric, liver, and gallbladder carcinomas have elevated serum DcR3 levels (>20 pg/mL) [23]. Furthermore, an association between DcR3 expression and tumor progression is well documented [26]. All of these observations suggest that DcR3 is involved in the immune evasion of malignant tumors. Therefore, to apply LIGHT as a cancer immunotherapeutic agent, it is necessary to create a LIGHT mutant binding to LTβR and HVEM, but not to DcR3.

In the past decade, several receptor-selective mutant proteins have been constructed, which are useful for functional analysis and as therapeutic agents. However, traditional point mutation methods are labor intensive because a large number of candidates must be individually assessed; therefore, successfully isolating the desired mutants has been difficult. We previously developed a modified phage display technique that can be used to create desired functional mutant proteins [27,28]. Using this technique, we have successfully created many mutant proteins with high bioactivity, high *in vivo* stability, or antagonist activity that are suitable as drug candidates [29–33].

In this study, we attempted to create an LTβR- and HVEM-specific LIGHT mutant with DcR3-evading capacity by phage display.

2. Materials and methods

2.1. Cells

The HT29.14S cell line, a clone of HT29 colon adenocarcinoma and sensitive to the pro-apoptotic activity of LIGHT, was kindly provided by Dr. Carl Ware (La Jolla Institute for Allergy and Immunology, CA) [34]. HT29.14S cells were cultured in Dulbecco's Modified Eagle's Medium (Wako Pure Chemical Industries, Osaka, Japan) supplemented with 10% fetal bovine serum, 10 mM HEPES, and antibiotics.

2.2. Library construction

Human LIGHT cDNA was kindly provided by Dr. K. Tamada (University of Maryland, Baltimore, MD). We used pY03′-LIGHT, in which the C-terminus of the extracellular domain region of the LIGHT sequence (encoding amino acids Gly66 to Val240) is fused to the N-terminus of the M13 phage G3P, as a template to generate double-stranded DNA fragments of LIGHT by PCR. PCR amplification was performed using primers containing the sequence NNS (which encodes all 20 standard amino acids) at Glu115, Thr116, Gln117, Leu118, Gly119, and Leu120 of LIGHT. The PCR products were digested with NcoI and ApaI and then ligated into the phagemid vector pY03′. The resultant phagemid was electroporated into *Escherichia coli* (*E. coli*) TG1 cells (Stratagene, Cedar Creek, TX), yielding 7×10^7 independent clones. The phage library displaying LIGHT mutants was prepared as previously described [31]. Briefly, pY03′-transforming TG1 cells were infected with M13KO7 helper phage (Invitrogen, Carlsbad, CA) and cultured for 6 h at 37 °C. The resultant phage particles were precipitated from the culture supernatant by using polyethylene glycol (MP Biomedicals, Solon, OH) and resuspended in NTE buffer (100 mM NaCl, 10 mM Tris, 1 mM EDTA).

2.3. Selection and screening of receptor-selective LIGHT mutants by biopanning

An immunoplate was coated with 100 μL of soluble human LTβR–Fc chimera (R&D Systems, Minneapolis, MN) at 10 μg/mL in 50 mM bicarbonate buffer (pH 9.5), and blocked with blocking buffer (Sigma–Aldrich, St. Louis, MO). One hundred microliters of the prepared phage library was allowed to bind to immobilized LTβR for 2 h at room temperature. After 10 rounds of washing with phosphate-buffered saline (PBS; pH 7.4) containing 0.05% Tween 20, and subsequently once with PBS, bound phages were eluted with 150 μL 10 mM glycine–HCl (pH 2.0) for 5 min at 4 °C. After neutralization with 75 μL 1 M Tris–HCl (pH 8.0), the eluted phages were used to infect TG1 cells, and used for the second round of panning. After the second panning, single ampicillin-resistant colonies were picked and used to inoculate 500 μL of 2-YT containing 100 μg/mL ampicillin and 2% glucose in deep 96-well plates. The plates were incubated in a shaker at 37 °C for several hours until the OD_{600} of the cultures became approximately 0.5. We then added 10^8 plaque-forming units of M13KO7 helper phage to each well, and incubated the plates for 30 min at 37 °C without shaking, followed by an additional 30 min in a shaker, at 37 °C. The cells in each well were centrifuged and resuspended in 1 mL 2-YT containing 100 μg/mL ampicillin and 50 μg/mL kanamycin. Cultures were incubated in a shaker at 25 °C for 6 h. The resulting phage-containing culture supernatant, which was mixed with an equal volume of 2-fold concentrations of blocking buffer, was used for screening by enzyme-linked immunosorbent assay (ELISA) using LTβR–Fc-, HVEM–Fc-, or DcR3–Fc (R&D Systems)-immobilized plates. The levels of bound phage were detected by ELISA with mouse anti-M13 antibody–HRP (GE Healthcare, Buckinghamshire, UK). The DNA sequences of highly bound phage clones were analyzed by an ABI Prism 3100 (Applied Biosystems, Foster City, CA).

2.4. Expression and purification of recombinant LIGHTs

Production of LIGHT protein by using *E. coli* BL21(DE3) (Stratagene) was performed as described previously [12]. Briefly, BL21(DE3) cells harboring the expression plasmid pET15b-LIGHTs (amino acids Gly66–Val240) were incubated in Terrific Broth including 1 mM isopropyl β-D-1-thiogalactopyranoside, and the resultant inclusion bodies were washed, solubilized, and reduced by the methods previously described [12]. Then, the solubilized LIGHT was refolded by 100-fold dilution in a refolding buffer for 36 h at 4 °C. After dialysis against a buffer containing 20 mM Tris–HCl (pH 7.4) and 100 mM urea, active trimeric LIGHT proteins were purified by passage through a HiPrep Sephacryl S-100 HR column (GE Healthcare) following ion-exchange chromatography (Q Sepharose Fast Flow; GE Healthcare).

2.5. Cytotoxicity assay

HT29.14S cells (5000 cells/well) were incubated for 12 h at 37 °C. The cells were then incubated at 37 °C with serial dilutions of LIGHT protein in the presence of 40 units/mL human IFN-γ (R&D Systems). After 72 h, cell viability was assessed by WST-8 assay according to the manufacturer's instructions (Nacalai Tesque, Kyoto, Japan). The $OD_{450-650}$ was measured in a multiwell spectrophotometer (Molecular Devices, Inc., Tokyo, Japan). For the competition effect of DcR3, HT29.14S cells were incubated at 37 °C in the presence of 10 ng/mL LIGHTs and 40 units/mL human IFN-γ in one of a series of DcR3 concentration or incubated in the presence of 200 ng/mL DcR3 and 40 units/mL human IFN-γ in one of a series of LIGHT concentrations.

2.6. Analysis of binding kinetics by surface plasmon resonance (SPR)

The binding kinetics of LIGHTs were analyzed and compared by surface Plasmon resonance (BIAcore 2000, GE Healthcare). Human LTβR, HVEM, or DcR3–Fc chimera (R&D Systems) was diluted to 50 μg/mL in 10 mM sodium acetate (pH 4.5) and immobilized onto a CM5 sensor chip by using an amine coupling kit (GE Healthcare) as described [12]. During the association phase, LIGHTs diluted in HBS-EP running buffer (GE Healthcare) to 35, 17.5, 8.8, 4.4, or 2.2 nM were passed over the immobilized receptors for 2 min at a flow rate of 20 μL/min. During the dissociation phase, HBS-EP was run over the sensor chip for 1 min at a flow rate of 20 μL/min. Complexes were eluted by using 20 μL 10 mM glycine–HCl (pH 2.0). Data were evaluated by using BIAevaluation 4.1 software (GE Healthcare) to apply a 1:1 Langmuir binding model. The obtained sensorgrams were fitted globally over the range of injected concentrations and simultaneously over the association and dissociation phases.

3. Results

3.1. Library construction and selection of receptor-selective LIGHT mutants

The crystal structures of LIGHT, LTβR, and DcR3 have not been clarified, and the precise receptor binding residues of LIGHT are unclear. Rooney et al. using a three-dimensional model suggested that the A–A′ loop motif constructed of Glu115 and Leu120 residues is an important region for the receptor binding of LIGHT [34]. Therefore, to create receptor-specific LIGHT mutants with reduced ability to bind to DcR3, we constructed a phage library displaying

Table 1
Substituted residues of LIGHT mutants from A–A′ loop library.

No.	Amino acid residue					
	115	116	117	118	119	120
wtLIGHT	E	T	Q	L	G	L
1	T	N	T	S	K	S
2	H	T	V	H	G	L
3	L	L	G	S	A	E
4	L	R	I	N	P	L
5	H	A	H	A	H	Q
6	M	H	T	L	L	A
7	S	R	P	S	H	R
8	P	I	M	L	I	A
9	D	E	P	H	H	E
10	T	H	A	T	S	M

structural variants of LIGHT with randomized sequences at 6 amino acid residues of the A–A′ motif (amino acid positions Glu115, Thr116, Gln117, Leu118, Gly119, and Leu120). For the construction of the phage library, PCR was performed to replace these amino acids randomly with an NNS sequence. NNS covers all 20 amino acids (where N and S represent A/C/G/T and C/G, respectively). As a result, we constructed a library with 7×10^7 clones (>theoretical value; 20^6) (data not shown). Sequence analysis of randomly selected clones indicated that this library was composed of independent clones (Table 1).

For selection of LIGHT mutants with binding affinity to LTβR, two rounds of affinity panning using human LTβR were performed with the constructed phage library. Potent binders to LTβR were concentrated in the library through this panning procedure. We then screened the clones with binding specificity to LTβR and HVEM, but not DcR3. To isolate the desired clones, we analyzed the binding affinity of monoclonal clones in the concentrated phage library for each of the three receptors (Fig. 1). Many of the phage clones were strongly bound to LTβR and HVEM compared to wtLIGHT, whereas they showed lower affinity for DcR3 than wtLIGHT. In addition, interestingly, many clones strongly bound to LTβR tended to also bind to HVEM, and clones with low affinity to LTβR tended to also bind to HVEM weakly. On the other hand, the binding affinity for DcR3 tended to be independent of the affinity for LTβR and HVEM.

Next, to isolate receptor-selective LIGHT mutants with sufficient affinity for LTβR and HVEM, we selected the 42 clones with the highest affinity (about 2-fold higher) for both LTβR and HVEM in phage ELISA. We then calculated the binding specificity for LTβR/DcR3 (Fig. 2A) and HVEM/DcR3 (Fig. 2B) from the phage ELISA data.

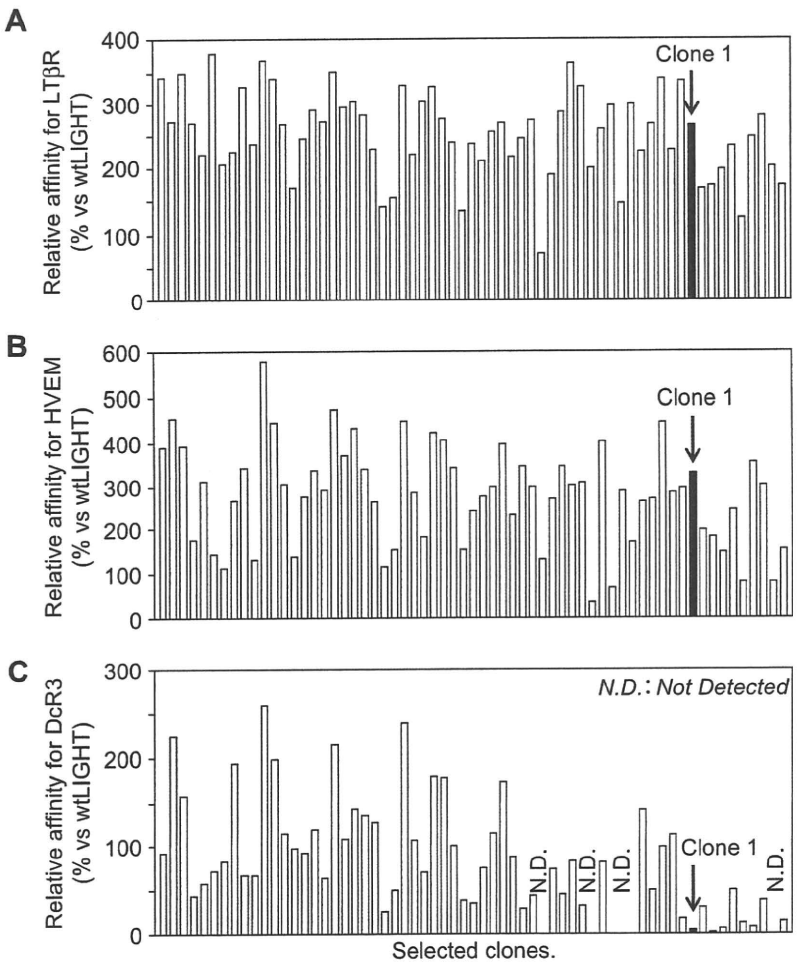

Fig. 1. Binding activity of selected phage clones to LTβR, HVEM, and DcR3. After second panning on LTβR, the binding properties to (A) LTβR, (B) HVEM, and (C) DcR3 of 63 selected phage clones were measured by ELISA. Relative affinity percentages were calculated as follows: (sample OD/positive control OD) × 100%. The positive control was the wtLIGHT-expressing phage.

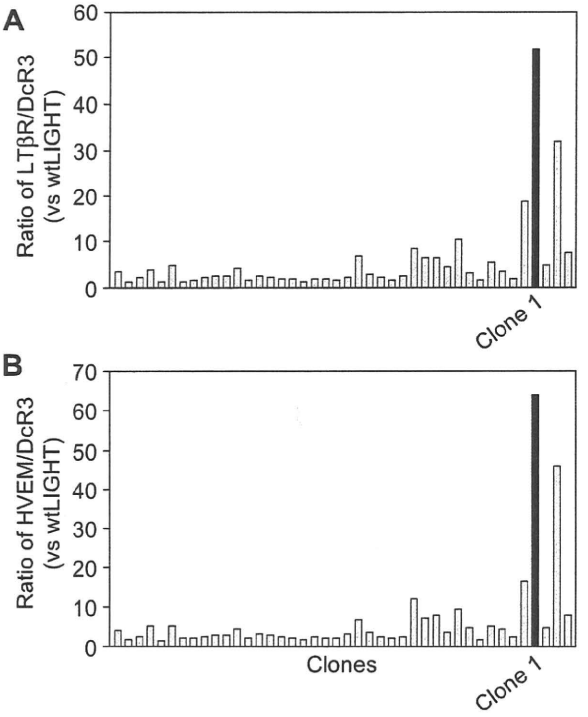

Fig. 2. Screening of DcR3-evading LIGHT mutants. Forty-two phage clones with more than 2-fold binding activity to both LTβR and HVEM were selected. Then, the receptor selectivity of the selected phages to (A) LTβR/DcR3 and (B) HVEM/DcR3 were calculated from the phage ELISA data. Black bar represents the LIGHT mutant-clone 1.

As a result, we found a clone (clone 1) that has the strongest binding selectivity for both LTβR and HVEM among the selected clones. In the same way, we obtained other 5 candidates for a DcR3-evading LIGHT mutant (data not shown). We sequenced these clones and found that Thr116 and Gly119 were identical to those of the wtLIGHT in almost all LIGHT mutants (Table 2). Furthermore, in all clones of the selected candidates, amino acid Leu at position 118 was changed to Gly.

3.2. Receptor selectivity of LIGHT mutant

To investigate the properties of receptor-selective LIGHT mutants in detail, we prepared recombinant proteins of the selected candidates. LIGHT protein was generated by truncation of the N-terminal 65 amino acids, which removes the cytoplasmic and transmembrane domains. We have confirmed that non-glycosylated LIGHT expressed in *E. coli* had the same bioactivity and receptor binding capacity compared to LIGHT expressed in mammalian cells, although LIGHT has a single N-linked glycosylation site (Asn102) [12]. So, in this study, we manufactured LIGHT mutants in *E. coli* as previously described [12]. LIGHT mutants expressed as inclusion bodies in *E. coli* were denatured and refolded. The refolded LIGHT mutants were then purified by ion-exchange and gel-filtration chromatography. As with wtLIGHT, we confirmed by using gel-filtration analysis that LIGHT mutants formed trimers, indicating that mutations did not affect trimer formation (data not shown). The purity of LIGHT mutants was greater than 95% confirmed by SDS-PAGE analysis (data not shown).

Next, to assess the receptor selectivity of LIGHT mutants, we measured their binding kinetics to LTβR, HVEM, and DcR3 by the SPR method (Table 3). The K_D values (the index of associative strength) of LIGHT mutants to LTβR and HVEM were almost same as those of wtLIGHT, with the exception of clone 5, indicating that LIGHT mutants showed almost the same affinity for LTβR and HVEM as wtLIGHT. In contrast, the K_D of LIGHT mutants to DcR3 was approximately 10-fold higher than that of wtLIGHT, indicating the dramatic loss of binding capacity to DcR3. Furthermore, detailed analysis of the kinetics indicated that the reduction in affinity of LIGHT mutants for DcR3 was due to an increase in dissociation rate constant (k_{off}) compared to wtLIGHT (Table 3). These data suggest that LIGHT mutants interact with DcR3 by rapid dissociation and show receptor selectivity for LTβR and HVEM.

3.3. Bioactivities of receptor-selective LIGHT mutants

To assess the bioactivity of LIGHT mutants, we performed cytotoxicity assays using HT29.14S cells, a clone sensitive to the pro-apoptotic effect of LIGHT (Fig. 3). In HT29.14S cells, cytotoxicity to wtLIGHT and LIGHT mutants was dose-dependent and the bioactivity of LIGHT mutant-clone 1 and -clone 4 was almost the same as that of wtLIGHT. In light of these data, we focused on LIGHT mutant-clone 1 because it showed the best bioactivity and DcR3-evading capacity among clones 1–6. To investigate the capacity of LIGHT mutant-clone 1 for evading the inhibition effects of DcR3, we examined the bioactivity of clone 1 by cytotoxicity assays using HT29.14S cells in the presence of DcR3 (Fig. 4). First, HT29.14S cells were incubated with serial dilutions of wtLIGHT or LIGHT mutant-clone 1 in the presence of DcR3 (200 ng/mL): lower doses of LIGHT mutant-clone 1 than wtLIGHT were cytotoxic (Fig. 4A). We also incubated HT29.14S cells with LIGHTs (10 ng/mL) in a DcR3 concentration series: wtLIGHT-induced cell death was blocked by DcR3 in a dose-dependent manner, with a 50% inhibitory concentration (IC_{50}) of 70 ng/mL, while the IC_{50} of DcR3 against clone 1

Table 2
Nucleotide and amino acid sequences of 6 candidates of DcR3-evading LIGHT mutants.

	Amino acid residue					
	115	116	117	118	119	120
wtLIGHT	E(GAG)	T(ACT)	Q(CAG)	L(CTG)	G(GGC)	L(CTG)
Clone 1	L(CTG)	T(ACC)	T(ACC)	G(GGC)	G(GGG)	N(AAC)
Clone 2	T(ACG)	T(ACC)	S(AGC)	G(GGC)	G(GGC)	N(AAC)
Clone 3	N(AAC)	T(ACC)	P(CCC)	G(GGC)	G(GGC)	H(CAC)
Clone 4	N(AAC)	S(ACG)	K(AAG)	G(GGG)	G(GGC)	H(CAC)
Clone 5	T(ACC)	T(ACC)	K(AAG)	G(GGC)	G(GGG)	T(ACC)
Clone 6	N(AAC)	T(ACC)	H(CAC)	G(GGC)	G(GGC)	N(AAC)

Table 3
Binding kinetics of LIGHT mutants to LTβR, HVEM and DcR3. Binding affinities to LTβR, HVEM or DcR3 were analyzed by surface plasmon resonance using a BIAcore 2000 instrument. Each kinetic parameter was calculated from the respective sensorgram using BIAevaluation 4.1 software.

	LTβR	HVEM	DcR3			
	K_D[a] (nM)	K_D[a] (nM)	k_{on}[b] (10^5/Ms)	k_{off}[c] (10^{-4}/s)	K_D[a] (nM)	Affinity[d] (% vs wtLIGHT)
wtLIGHT	1.30	1.50	3.3	2.0	0.6	100.0
Clone 1	1.80	2.15	4.8	27.5	5.7	10.7
Clone 2	1.63	1.25	3.4	24.2	18.7	3.3
Clone 3	1.77	1.36	4.2	18.4	4.7	13.1
Clone 4	1.89	2.11	4.5	20.2	4.6	13.3
Clone 5	2.54	6.60	1.9	17.3	8.9	6.8
Clone 6	1.90	1.63	4.8	22.0	4.6	13.0

[a] K_D is the equilibrium dissociation constant.
[b] k_{on} is the association kinetic constant.
[c] k_{off} is the dissociation kinetic constant.
[d] Relative affinity values were calculated as 100 × K_D (wtLIGHT)/K_D (LIGHT mutant).

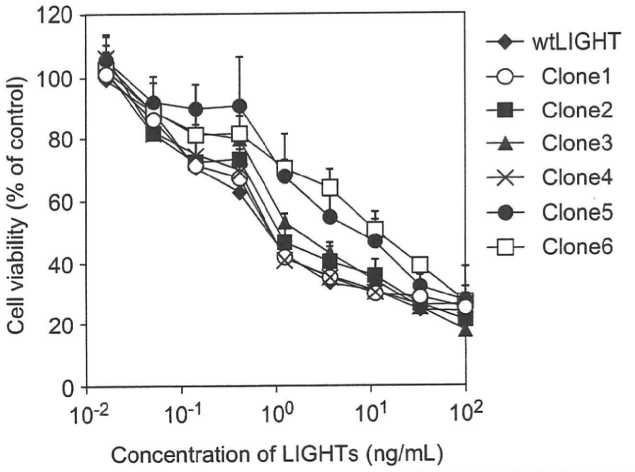

	wtLIGHT	Clone1	Clone2	Clone3	Clone4	Clone5	Clone6
EC50 (ng/mL)	0.73	0.83	1.29	2.20	0.90	5.70	10.9

Fig. 3. Cytotoxic effects of wtLIGHT and LIGHT mutants on HT29.14S cells. The bioactivities of LIGHTs were measured in cytotoxicity assays. HT29.14S cells were incubated with serial dilutions of wtLIGHT or LIGHT mutants in the presence of 40 units/mL IFN-γ. After 72 h incubation, cell viability was assessed by WST-8 assay. Each data point represents the mean ± SD. The EC_{50} is the concentration of LIGHT required to inhibit cell viability by 50%.

was 4329 ng/mL (Fig. 4B). These data indicate that the DcR3-evading capacity of LIGHT mutant-clone 1 was more than 62-fold higher than that wtLIGHT.

4. Discussion

LIGHT has potent anti-tumor activities through the activation of immune response, and is a promising candidate for cancer immunotherapy. However, there is strong evidence that DcR3 is over-expressed in various tumors. DcR3 neutralizes the biological effects of LIGHT and contributes to immune escape of tumors by binding to LIGHT. Therefore, to develop more efficient cancer immunotherapy by LIGHT, it is necessary to create LIGHT mutants with DcR3-evading capacity.

In this study, we attempted to create a receptor-selective LIGHT mutant without the capacity of binding to DcR3. Two loop regions

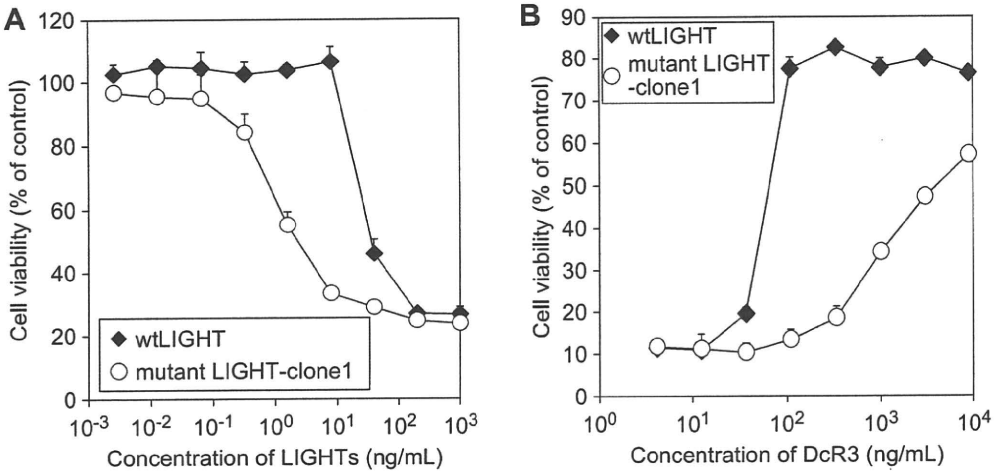

	IC50 (ng/mL)	Relative DcR3-evading capacity (%)
wtLIGHT	70	100
Clone1	4330	6185

Fig. 4. Effect of DcR3 on LIGHT-mediated apoptosis in human HT29.14S cells. (A) HT29.14S cells were incubated with serial dilutions of wtLIGHT or LIGHT mutant-clone 1 in the presence of 200 ng/mL DcR3 and 40 units/mL IFN-γ. After 72 h incubation, cell viability was assessed by WST-8 assay. (B) HT29.14S cells were incubated with LIGHT (10 ng) in the presence of various concentrations of DcR3 with 40 units/mL IFN-γ. After 72 h incubation, cell viability was assessed by WST-8 assay. Each data point represents the mean ± SD. The IC_{50} is the concentration of DcR3 required to inhibit the cytotoxicity of LIGHT by 50%.

located on opposite sides of the LIGHT subunit have been suggested as putative receptor binding sites of LIGHT [34,35]. In this study, we selected the A–A′ loop between Glu115 and Leu120, and constructed a phage library displaying structural variants of LIGHT with randomized sequences at the 6 amino acids residues there. After panning and selection, we identified 6 mutants as candidates for receptor-selective LIGHT mutants. Sequence analysis revealed that Gly119 in all LIGHT mutants was identical to that of wtLIGHT (Table 2), which is consistent with the previously reported idea that Gly119 plays critical roles in maintaining receptor binding of LIGHT to LTβR and HVEM [34]. In addition, in almost all LIGHT mutants we found that Thr116 was also identical to that of the wtLIGHT. Since almost all LIGHT mutants that bound to both LTβR and HVEM in phage ELISA lacked mutations at Thr116 (data not shown), we conclude that Thr116 is important for receptor binding of LIGHT. Furthermore, in all clones with low affinity for DcR3, the amino acid Leu at position 118 was changed to Gly (Table 2). These results indicate that Thr116 and Gly119 play a critical role in binding to LTβR and HVEM, and that Leu118 might be involved in the LIGHT–DcR3 association.

Next, we measured the binding affinity of the LIGHT clones for LTβR, HVEM, and DcR3 by the SPR method (Table 3). Interestingly, LIGHT mutants showed approximately 10-fold lower affinity to DcR3 than wtLIGHT because of a faster off-rate compared to wtLIGHT, while the K_D of LIGHT mutants to LTβR and HVEM was almost same as that of wtLIGHT. These data suggest that LIGHT mutants interact with DcR3 by rapid dissociation and show the receptor selectivity to LTβR and HVEM. Furthermore, competition assay using DcR3 showed that LIGHT mutant-clone 1 was 60-fold more resistant to the neutralization effect of DcR3 compared to wtLIGHT, while LIGHT mutant-clone 1 has almost same biological activity as wtLIGHT. From these data, we consider that LIGHT mutant-clone 1 might be a superior candidate for cancer therapy.

In this study, we concentrated phages expressing LIGHT mutants by simple affinity panning for LTβR, but not competitive panning using DcR3, because the association mode of LIGHT between LTβR, HVEM, and DcR3 was unclear. Our data suggest that the A–A′ loop motif (Glu115–Leu120 residues) of LIGHT plays an important role in binding to all three receptors and exhibits a similar association mode with LTβR and HVEM, while the association mode with DcR3 might be different from that of LTβR and HVEM. This indicates that competitive panning using DcR3 is more promising to isolate more receptor-selective clones. On the other hand, our preliminary data indicated that the G–H loop motif (amino acids at positions Glu222, Arg223, Arg226, Leu227, Arg228, and Asp229) of LIGHT plays an important role in binding to LTβR and HVEM (data not shown). These data are informative for construction of desired functional mutant LIGHTs with receptor selectivity and high bioactivity, among other advantageous characteristics.

Nomura et al. recently reported a method for generating functional mutant proteins (gene shuffling method) [36]. This method enables the creation of mutant proteins with mutations in two or more loop motifs that also retain the binding characteristic of each library. So, we speculate that the construction of an A–A′ and G–H loop library by the gene shuffling method might enable us to create an LTβR- or HVEM-selective LIGHT mutant that is useful for the functional analysis of LTβR or HVEM.

5. Conclusions

Here, we created fully bioactive DcR3-evading LIGHT mutants by using a phage display technique and clarified the molecular basis of its receptor selectivity. A better understanding of the correlation between structure, kinetic behavior, and activity will likely accelerate drug discovery because of increased awareness of the properties of therapeutic proteins. We suggest that LIGHT mutants, at least LIGHT mutant-clone 1, might be a powerful tool for cancer therapy, and we believe that our data offer valuable information for the construction of even more functional LIGHT mutants.

Acknowledgements

The authors declare that they have no conflict of interests. This study was supported in part by grants from the Ministry of Health, Labor, and Welfare in Japan; by the Research on Health Sciences focusing on Drug Innovation from the Japan Health Sciences Foundation; and by the Takeda Science Foundation.

References

[1] Mauri DN, Ebner R, Montgomery RI, Kochel KD, Cheung TC, Yu GL, et al. LIGHT, a new member of the TNF superfamily, and lymphotoxin alpha are ligands for herpesvirus entry mediator. Immunity 1998;8:21–30.
[2] Harrop JA, McDonnell PC, Brigham-Burke M, Lyn SD, Minton J, Tan KB, et al. Herpesvirus entry mediator ligand (HVEM-L), a novel ligand for HVEM/TR2, stimulates proliferation of T cells and inhibits HT29 cell growth. J Biol Chem 1998;273:27548–56.
[3] Murphy M, Walter BN, Pike-Nobile L, Fanger NA, Guyre PM, Browning JL, et al. Expression of the lymphotoxin beta receptor on follicular stromal cells in human lymphoid tissues. Cell Death Differ 1998;5:497–505.
[4] Stopfer P, Mannel DN, Hehlgans T. Lymphotoxin-beta receptor activation by activated T cells induces cytokine release from mouse bone marrow-derived mast cells. J Immunol 2004;172:7459–65.
[5] Yu P, Lee Y, Liu W, Chin RK, Wang J, Wang Y, et al. Priming of naive T cells inside tumors leads to eradication of established tumors. Nat Immunol 2004;5:141–9.
[6] Tamada K, Shimozaki K, Chapoval AI, Zhai Y, Su J, Chen SF, et al. LIGHT, a TNF-like molecule, costimulates T cell proliferation and is required for dendritic cell-mediated allogeneic T cell response. J Immunol 2000;164:4105–10.
[7] Yu P, Fu YX. Targeting tumors with LIGHT to generate metastasis-clearing immunity. Cytokine Growth Factor Rev 2008;19:285–94.
[8] Lukashev M, LePage D, Wilson C, Bailly V, Garber E, Lukashin A, et al. Targeting the lymphotoxin-beta receptor with agonist antibodies as a potential cancer therapy. Cancer Res 2006;66:9617–24.
[9] Zhai Y, Guo R, Hsu TL, Yu GL, Ni J, Kwon BS, et al. LIGHT, a novel ligand for lymphotoxin beta receptor and TR2/HVEM induces apoptosis and suppresses in vivo tumor formation via gene transfer. J Clin Invest 1998;102:1142–51.
[10] Loeffler M, Le'Negrate G, Krajewska M, Reed JC. Attenuated *Salmonella* engineered to produce human cytokine LIGHT inhibit tumor growth. Proc Natl Acad Sci U S A 2007;104:12879–83.
[11] Zhang J, Wang Q, Zhao D, Cao X. Induction of potent anti-tumor immunity by direct injection of Ad-LIGHT at the site of tumor inoculation. Cytotherapy 2007;9:386–96.
[12] Morishige T, Yoshioka Y, Inakura H, Tanabe A, Watanabe H, Yao X, et al. LIGHT protein suppresses tumor growth by augmentation of immune response. Immunol Lett 2009;127:33–8.
[13] Morishige T, Yoshioka Y, Tanabe A, Yao X, Mizuguchi H, Tsunoda SI, et al. Comparison of the anti-tumor activity of naïve, secreted, and membrane-bound LIGHT in mouse tumor models. Int Immunopharmacol 2010;10:26–33.
[14] Pitti RM, Marsters SA, Lawrence DA, Roy M, Kischkel FC, Dowd P, et al. Genomic amplification of a decoy receptor for Fas ligand in lung and colon cancer. Nature 1998;396:699–703.
[15] Zhang J, Salcedo TW, Wan X, Ullrich S, Hu B, Gregorio T, et al. Modulation of T-cell responses to alloantigens by TR6/DcR3. J Clin Invest 2001;107:1459–68.
[16] Yu KY, Kwon B, Ni J, Zhai Y, Ebner R, Kwon BS. A newly identified member of tumor necrosis factor receptor superfamily (TR6) suppresses LIGHT-mediated apoptosis. J Biol Chem 1999;274:13733–6.
[17] Migone TS, Zhang J, Luo X, Zhuang L, Chen C, Hu B, et al. TL1A is a TNF-like ligand for DR3 and TR6/DcR3 and functions as a T cell costimulator. Immunity 2002;16:479–92.
[18] Gill RM, Hunt JS. Soluble receptor (DcR3) and cellular inhibitor of apoptosis-2 (cIAP-2) protect human cytotrophoblast cells against LIGHT-mediated apoptosis. Am J Pathol 2004;165:309–17.
[19] Hayashi S, Miura Y, Nishiyama T, Mitani M, Tateishi K, Sakai Y, et al. Decoy receptor 3 expressed in rheumatoid synovial fibroblasts protects the cells against Fas-induced apoptosis. Arthritis Rheum 2007;56:1067–75.
[20] Tsuji S, Hosotani R, Yonehara S, Masui T, Tulachan SS, Nakajima S, et al. Endogenous decoy receptor 3 blocks the growth inhibition signals mediated by Fas ligand in human pancreatic adenocarcinoma. Int J Cancer 2003;106:17–25.
[21] Ohshima K, Haraoka S, Sugihara M, Suzumiya J, Kawasaki C, Kanda M, et al. Amplification and expression of a decoy receptor for fas ligand (DcR3) in virus (EBV or HTLV-I) associated lymphomas. Cancer Lett 2000;160:89–97.

[22] Bai C, Connolly B, Metzker ML, Hilliard CA, Liu X, Sandig V, et al. Over-expression of M68/DcR3 in human gastrointestinal tract tumors independent of gene amplification and its location in a four-gene cluster. Proc Natl Acad Sci U S A 2000;97:1230–5.
[23] Wu Y, Han B, Sheng H, Lin M, Moore PA, Zhang J, et al. Clinical significance of detecting elevated serum DcR3/TR6/M68 in malignant tumor patients. Int J Cancer 2003;105:724–32.
[24] Wu Y, Guo E, Yu J, Xie Q. High DcR3 expression predicts stage pN2-3 in gastric cancer. Am J Clin Oncol 2008;31:79–83.
[25] Chen G, Luo D. Over-expression of decoy receptor 3 in gastric precancerous lesions and carcinoma. Ups J Med Sci 2008;113:297–304.
[26] Macher-Goeppinger S, Aulmann S, Wagener N, Funke B, Tagscherer KE, Haferkamp A, et al. Decoy receptor 3 is a prognostic factor in renal cell cancer. Neoplasia 2008;10:1049–56.
[27] Yamamoto Y, Tsutsumi Y, Yoshioka Y, Nishibata T, Kobayashi K, Okamoto T, et al. Site-specific PEGylation of a lysine-deficient TNF-alpha with full bioactivity. Nat Biotechnol 2003;21:546–52.
[28] Mukai Y, Yoshioka Y, Tsutsumi Y. Phage display and PEGylation of therapeutic proteins. Comb Chem High Throughput Screen 2005;8:145–52.
[29] Yoshioka Y, Tsutsumi Y, Ikemizu S, Yamamoto Y, Shibata H, Nishibata T, et al. Optimal site-specific PEGylation of mutant TNF-alpha improves its antitumor potency. Biochem Biophys Res Commun 2004;315:808–14.
[30] Shibata H, Yoshioka Y, Ikemizu S, Kobayashi K, Yamamoto Y, Mukai Y, et al. Functionalization of tumor necrosis factor-alpha using phage display technique and PEGylation improves its antitumor therapeutic window. Clin Cancer Res 2004;10:8293–300.
[31] Shibata H, Yoshioka Y, Ohkawa A, Minowa K, Mukai Y, Abe Y, et al. Creation and X-ray structure analysis of the tumor necrosis factor receptor-1-selective mutant of a tumor necrosis factor-alpha antagonist. J Biol Chem 2008;283:998–1007.
[32] Shibata H, Yoshioka Y, Ohkawa A, Abe Y, Nomura T, Mukai Y, et al. The therapeutic effect of TNFR1-selective antagonistic mutant TNF-alpha in murine hepatitis models. Cytokine 2008;44:229–33.
[33] Kayamuro H, Abe Y, Yoshioka Y, Katayama K, Nomura T, Yoshida T, et al. The use of a mutant TNF-alpha as a vaccine adjuvant for the induction of mucosal immune responses. Biomaterials 2009;30:5869–76.
[34] Rooney IA, Butrovich KD, Glass AA, Borboroglu S, Benedict CA, Whitbeck JC, et al. The lymphotoxin-beta receptor is necessary and sufficient for LIGHT-mediated apoptosis of tumor cells. J Biol Chem 2000;275:14307–15.
[35] Chen MC, Hwang MJ, Chou YC, Chen WH, Cheng G, Nakano H, et al. The role of apoptosis signal-regulating kinase 1 in lymphotoxin-beta receptor-mediated cell death. J Biol Chem 2003;278:16073–81.
[36] Nomura T, Abe Y, Kamada H, Inoue M, Kawara T, Arita S, et al. Novel protein engineering strategy for creating highly receptor-selective mutant TNFs. Biochem Biophys Res Commun 2009;388:667–71.

Biochemical and Biophysical Research Communications 393 (2010) 888–893

Contents lists available at ScienceDirect

Biochemical and Biophysical Research Communications

journal homepage: www.elsevier.com/locate/ybbrc

Creation of a lysine-deficient LIGHT mutant with the capacity for site-specific PEGylation and low affinity for a decoy receptor

Tomohiro Morishige [a,1], Yasuo Yoshioka [a,b,*,1], Hiroshi Inakura [a], Aya Tanabe [a], Xinglei Yao [a], Shin-ichi Tsunoda [c], Yasuo Tsutsumi [c,d], Yohei Mukai [a], Naoki Okada [a], Shinsaku Nakagawa [a,b,*]

[a] Laboratory of Biotechnology and Therapeutics, Graduate School of Pharmaceutical Sciences, Osaka University, 1-6 Yamadaoka, Suita, Osaka 565-0871, Japan
[b] The Center for Advanced Medical Engineering and Informatics, Osaka University, 1-6 Yamadaoka, Suita, Osaka 565-0871, Japan
[c] Laboratory of Pharmaceutical Proteomics, National Institute of Biomedical Innovation, 7-6-8 Saito-Asagi, Ibaraki, Osaka 567-0085, Japan
[d] Laboratory of Toxicology and Safety Science, Graduate School of Pharmaceutical Sciences, Osaka University, 1-6 Yamadaoka, Suita, Osaka 565-0871, Japan

ARTICLE INFO

Article history:
Received 10 February 2010
Available online 20 February 2010

Keywords:
Bioconjugation
Cancer immunotherapy
Cytokine
Kinetic analysis
Protein engineering
Receptor selectivity

ABSTRACT

The cytokine LIGHT is a promising candidate for cancer therapy. However, the therapeutic effect of LIGHT as a systemic anticancer agent is currently insufficient because of its instability and its binding to nonfunctional soluble decoy receptor 3 (DcR3), which is overexpressed in various tumors. Modification of proteins with polyethylene glycol (PEGylation) can improve their *in vivo* stability, but PEGylation may occur randomly at all lysine residues and the NH_2-terminus; therefore, PEGylated proteins are generally heterogeneous and have decreased bioactivity. In this study, we attempted to create a lysine-deficient LIGHT mutant that could be PEGylated site-specifically and would have lower affinity for DcR3. We prepared phage libraries expressing LIGHT mutants in which all the lysine residues were replaced with other amino acids. A lysine-deficient LIGHT mutant [mLIGHT-Lys(−)] was isolated by panning against lymphotoxin β receptor (LTβR). mLIGHT-Lys(−) could be site-specifically PEGylated at its NH_2-terminus, yielding molecular uniformity and *in vitro* bioactivity equal to that of non-PEGylated, wild-type LIGHT. Furthermore, mLIGHT-Lys(−) was not trapped by the nonfunctional DcR3, despite binding to its functional receptors. These results suggest that mLIGHT-Lys(−) might be a useful candidate for cancer therapy.

1. Introduction

The tumor necrosis factor (TNF) superfamily member LIGHT (homologous to lymphotoxins, shows inducible expression, and competes with herpes simplex virus glycoprotein D for herpesvirus entry mediator (HVEM), a receptor expressed by T lymphocytes) is a ligand for two functional cellular receptors, lymphotoxin β receptor (LTβR) and HVEM [1,2]. The LTβR signaling induces cytotoxicity against some human cancer cells, and promotes the release of chemokines that attract naive T cells to stromal cells [3,4]. LIGHT-HVEM signaling functions as a costimulatory molecule for T-cell activation [3,5]. Recently, Yu et al. showed that the transgenic expression of LIGHT in tumors efficiently induces systemic tumor immunity, leading to the rejection of primary and metastatic tumors in mice [4]. Therefore, LIGHT has attracted a great deal of attention as a potential agent for cancer immunotherapy. However, LIGHT further binds to a nonfunctional soluble decoy receptor 3 (DcR3). DcR3 is overexpressed in various tumors, including malignant tumors arising from the esophagus, stomach, lung, colon, and rectum [6–8]. An association between DcR3 expression and tumor progression has been well documented [9]. In addition, DcR3 acts as an inhibitory receptor for anticancer cytokines such as LIGHT and Fas ligand, among others [6,10,11]. Therefore, to apply LIGHT as a cancer immunotherapeutic agent, it will be necessary to create a LIGHT mutant that binds to LTβR and HVEM, but not to DcR3.

In addition, cytokines, including LIGHT, are generally highly unstable *in vivo*, limiting their clinical application. In fact, although intratumoral injection of LIGHT provides a significant therapeutic effect, systemic administration of LIGHT protein does not induce sufficient tumor suppression [12]. One of the most useful ways to enhance the stability of proteins is to conjugate them to polyethylene glycol (PEG) [13,14]. PEGylation of proteins increases their molecular size, enhances steric hindrance, and improves their plasma half-lives. The prolonged circulating lifetime in the blood induces the enhanced permeability and retention effect (EPR effect), which is based on the leaky nature of tumor blood vessels,

* Corresponding authors. Addresses: The Center for Advanced Medical Engineering and Informatics, Osaka University, 1-6 Yamadaoka, Suita, Osaka 565-0871, Japan. Fax: +81 6 6879 8177 (Y. Yoshioka); Laboratory of Biotechnology and Therapeutics, Graduate School of Pharmaceutical Sciences, Osaka University, 1-6 Yamadaoka, Suita, Osaka 565-0871, Japan. Fax: +81 6 6879 8179 (S. Nakagawa).
E-mail addresses: yasuo@phs.osaka-u.ac.jp (Y. Yoshioka), nakagawa@phs.osaka-u.ac.jp (S. Nakagawa).
[1] These authors contributed equally to this work.

0006-291X/$ - see front matter © 2010 Elsevier Inc. All rights reserved.
doi:10.1016/j.bbrc.2010.02.119

resulting in increased delivery of the conjugates to tumor tissue. In fact, our group has previously shown that optimal PEGylation of bioactive proteins such as TNFα improves their *in vivo* therapeutic potency [15–18].

PEGylation of proteins is conducted at the amino groups of lysine residues because they are highly reactive, and the PEGylation reaction is mild enough to minimize disruption of the protein structure. However, this PEGylation randomly occurs at the NH_2-terminus as well as all internal lysine residues, and the resulting conjugates show a significant loss of molecular uniformity and activity *in vitro*. Therefore, clinical application of PEGylated proteins has been limited in most cases, with the exception of some bioactive proteins such as interferon (IFN)-α [19]. We previously developed a modified phage display technique that can be used to create desired functional mutant proteins. Using this technique, we have successfully created a bioactive lysine-deficient mutant TNFα that enables NH_2-terminal-specific PEGylation [20]. The site-specific PEGylated mutant TNFα has comparable bioactivity to non-PEGylated wild-type TNFα *in vitro*, and other properties, including plasma half-life and antitumor activity, are greatly improved.

In this study, we used phage display to create a lysine-deficient LIGHT mutant with full bioactivity and uniform site-specific PEGylation. In addition, we investigated whether this LIGHT mutant had decreased binding to DcR3 to evaluate its usability for cancer therapy.

2. Materials and methods

2.1. Cells

The HT29.14S cell line, a clone of the HT29 colon adenocarcinoma sensitive to the pro-apoptotic activity of LIGHT, was kindly provided by Dr. Carl Ware (La Jolla Institute for Allergy and Immunology, La Jolla, CA) [21]. HT29.14s cells were cultured as described previously [22].

2.2. Library construction

A human LIGHT cDNA was kindly provided by Dr. K. Tamada (University of Maryland, Baltimore, MD) [5]. We used pY03′-LIGHT, in which the COOH-terminus of the extracellular domain region of the LIGHT sequence (encoding amino acids Gly66 to Val240) is fused to the NH_2-terminus of the M13 phage g3p, as a template to generate a double-stranded DNA fragment of LIGHT by PCR. Two-step PCR amplification was performed using three primers: Primer 1, 5′-CCCGCTGGGCCTGGCCAGCACCATCACCCACGGCCTCT ACNNSCGCACACCCCGCTACCCCGAGGAGCTG-3′; Primer 2, 5′-GTAAATGAATTTTCTGTATGAGG-3′; and Primer 3, 5′-TACCACGAT GGGGCCCTTGTGGTCACCNNSGCTGGCTACTACTACATCTACTCCNNS GTGCAGCTCGGCGGTGTGGGCTGCCCGCTGGGCCTGGCCAGCACCAT C-3′. These primers contain the sequence NNS (which encodes all 20 standard amino acids) at Lys137, Lys146, and Lys168 of LIGHT. The PCR products were ligated into the phagemid vector pY03′. The resultant phagemid was electroporated into *Escherichia coli* (*E. coli*) TG1 cells (Stratagene, Cedar Creek, TX), yielding 8×10^3 independent clones. The phage library displaying LIGHT mutants was prepared as previously described [23].

2.3. Selection of phages displaying lysine-deficient LIGHT mutant

Screening for lysine-deficient LIGHT mutants with high binding activity to LTβR was performed as described previously [22]. Briefly, an immunoplate was coated with a soluble human LTβR-Fc chimera (R&D, Minneapolis, MN), and the prepared phage library was allowed to bind to the immobilized LTβR. After the second round of panning, single colonies were picked and cultured. The resulting phage-containing culture supernatant was used for screening by ELISA against LTβR-Fc.

2.4. Expression and purification of recombinant LIGHTs

Production of LIGHT protein by using *E. coli* BL21(DE3) (Stratagene) was performed as described previously [12]. Briefly, BL21(DE3) cells harboring the plasmid pET15b-LIGHTs were incubated with isopropyl β-D-1-thiogalactopyranoside, and the resultant inclusion bodies were solubilized and refolded. After dialysis against a buffer containing Tris–HCl and urea, active trimeric LIGHT proteins were purified using ion-exchange chromatography (Q Sepharose Fast Flow; GE Healthcare, Buckinghamshire, UK) and HiPrep Sephacryl S-100 HR column (GE Healthcare).

2.5. Cytotoxicity assay

HT29.14S cells (5000 cells/well) were incubated for 12 h at 37 °C, and treated with serial dilutions of LIGHT protein in the presence of 40 U/mL human IFN-γ (R&D). For the competition assay against DcR3, HT29.14S cells were incubated with 10 ng/mL LIGHTs and 40 U/mL human IFN-γ in the presence of various concentrations of DcR3 (R&D). Seventy-two hours after the treatment, cell viability was assessed with a standard methylene blue assay method.

2.6. PEGylation of LIGHT

Wild-type LIGHT (wtLIGHT) and a lysine-deficient LIGHT mutant were reacted with methoxy-PEG-succinimidyl propionate with molecular weight 5000 (PEG5K; NEKTAR, San Carlos, CA) targeting total primary amine groups of each LIGHT at 37 °C for 10 min. Then, 10-fold molar excess of ε-aminocaproic acid (Sigma–Aldrich) relative to the PEG5K was added to stop the reaction. SDS–PAGE analysis of the PEGylated LIGHTs was conducted under reducing conditions, and the proteins in the gels were stained with Coomassie brilliant blue (CBB). The PEGylated LIGHTs were purified by size-exclusion chromatography (Superdex 200 pg; GE Healthcare).

2.7. Analysis of binding kinetics by surface plasmon resonance (SPR)

The binding kinetics of LIGHTs were analyzed with the SPR method as described previously (BIAcore 2000, GE Healthcare) [12]. Briefly, a human LTβR-, HVEM-, or DcR3-Fc chimera was immobilized onto a CM5 sensor chip (GE Healthcare). During the association phase, LIGHTs diluted in HBS-EP running buffer (GE Healthcare) were passed over the immobilized receptors. Data were evaluated by using BIAevaluation 4.1 software (GE Healthcare) using a 1:1 Langmuir binding model.

2.8. Statistical analysis

All results are presented as means ± standard deviation (SD). Differences were compared by using Student's *t*-tests.

3. Results and discussion

The aim of this study was to create lysine-deficient LIGHT mutants with full bioactivity and the ability for site-specific PEGylation. In addition, we further investigated the DcR3 evading capacity of LIGHT mutants to evaluate their usability for cancer therapy.

3.1. Library construction and selection of lysine-deficient LIGHT mutants

To create fully bioactive lysine-deficient LIGHT mutants with substitution of all three lysine residues, we constructed a phage library displaying structural variants of LIGHT with randomized amino acids at three lysine residues (Lys137, Lys146, and Lys168). The constructed phage library yielded 8×10^3 independent clones (data not shown). Then, to isolate lysine-deficient LIGHT mutants that retained the bioactivity of wtLIGHT, we performed two rounds of affinity panning using LTβR with the constructed phage library. Potent binders to LTβR were concentrated in the library through this panning procedure. We randomly picked phage clones before and after the panning procedure and assessed their binding affinity for LTβR by ELISA using phages in the culture supernatant (Fig. 1A). After panning, 11 of 33 positive clones had higher binding affinities for LTβR than wtLIGHT, whereas before panning only 1 out of 21 clones had higher affinity than wtLIGHT. To accurately evaluate the binding affinities of these positive clones for LTβR and HVEM, we examined the binding affinities of 11 clones after the panning using purified phages (Fig. 1B and C). Clones 2, 5, 9, and 11 had the same or higher affinity as wtLIGHT for both LTβR and HVEM. Furthermore, we analyzed the sequences of these 11 clones and identified clones 4, 6, 7, 8, and 11 as clones without an amber stop codon or a lysine residue at amino acid positions 137, 146, and 168 (Table 1). Collectively, these results indicated that clone 11 was a clone deficient in lysine residues with high binding affinities for both LTβR and HVEM. We selected clone 11 as lysine-deficient LIGHT mutant (mLIGHT-Lys(−)). We also note that Gly157 of clone 11 was unexpectedly substituted with aspartic acid (data not shown).

Table 1
Nucleotide and amino acid sequences of candidate lysine-deficient LIGHT mutants obtained after affinity panning for LTβR.

Clone	Position		
	K137	K146	K168
Clone 1	Amb (TAG)	M (ATG)	L (CTC)
Clone 2	S (TCG)	Amb (TAG)	L (TTG)
Clone 3	I (ATC)	Amb (TAG)	K (AAG)
Clone 4	Q (CAG)	L (CTC)	L (CTG)
Clone 5	T (ACC)	K (AAG)	K (AAG)
Clone 6	T (ACC)	G (GGC)	R (CGC)
Clone 7	R (CGG)	S (AGC)	L (TTG)
Clone 8	R (CGG)	L (CTG)	L (TTG)
Clone 9	K (AAG)	Amb (TAG)	L (TTG)
Clone 10	K (AAG)	L (CTC)	L (CTG)
Clone 11	R (AGG)	Q (CAG)	L (TTG)

3.2. Bioactivity of lysine-deficient mLIGHT-Lys(−) and affinity for DcR3

To investigate the properties of mLIGHT-Lys(−) in detail, we prepared recombinant mLIGHT-Lys(−) protein using an *E. coli* expression system, as previously described [12]. Gel-filtration analysis confirmed that mLIGHT-Lys(−) forms homotrimers, as wtLIGHT does (Fig. 2A). We confirmed that the purity of mLIGHT-Lys(−) was sufficiently high using SDS–PAGE analysis (Fig. 2B). Next, to assess the bioactivity of mLIGHT-Lys(−), we performed cytotoxicity assays using HT29.14S cells, a clone sensitive to the pro-apoptotic effect of LIGHT. The bioactivity of mLIGHT-Lys(−) was almost equal to that of wtLIGHT (Fig. 2C). Furthermore, to investigate the receptor binding properties of mLIGHT-Lys(−), we measured its binding kinetics for LTβR, HVEM, and DcR3 by

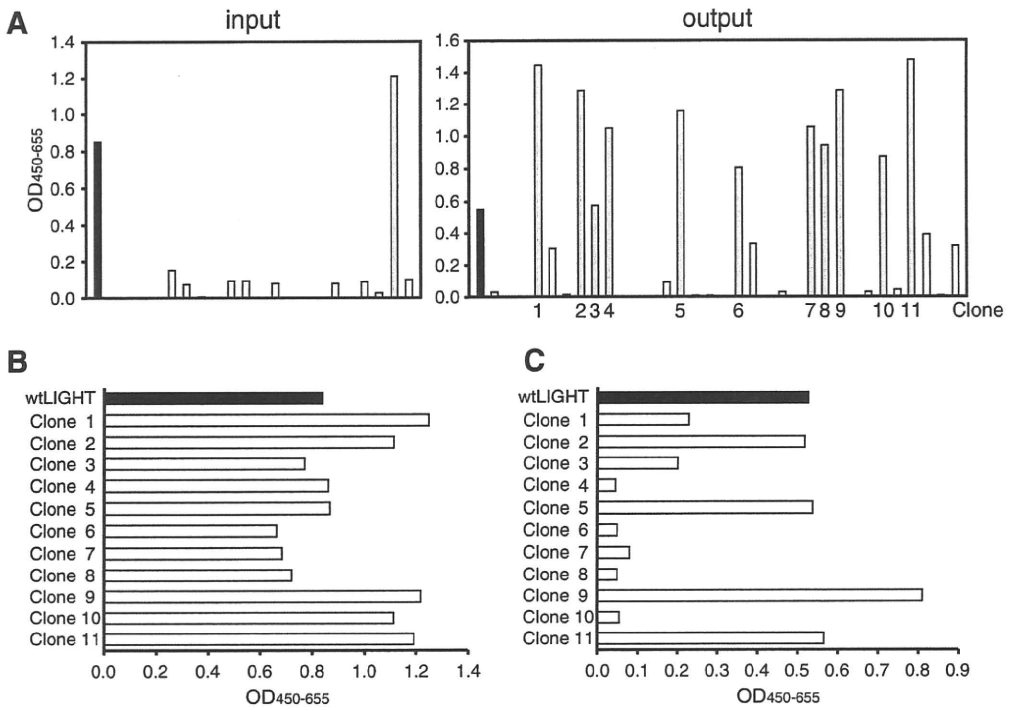

Fig. 1. Binding activity of selected phage clones to LTβR and HVEM. (A) Concentration of candidates with high binding affinity for LTβR through affinity panning. The binding properties of 21 (before panning, input) or 33 (after panning, output) randomly selected phage clones to LTβR were measured by ELISA using TG1 supernatants including each phage clone. Black bars represent the wtLIGHT-expressing phage, and gray bars represent the clones with higher binding affinity to LTβR than wtLIGHT-expressing phage. (B,C) Binding properties of the selected phage clones against LTβR or HVEM. Each LIGHT mutant-expressing phage was purified and applied to plates with immobilized LTβR (B) or HVEM (C). Then, the binding affinity was measured by ELISA.

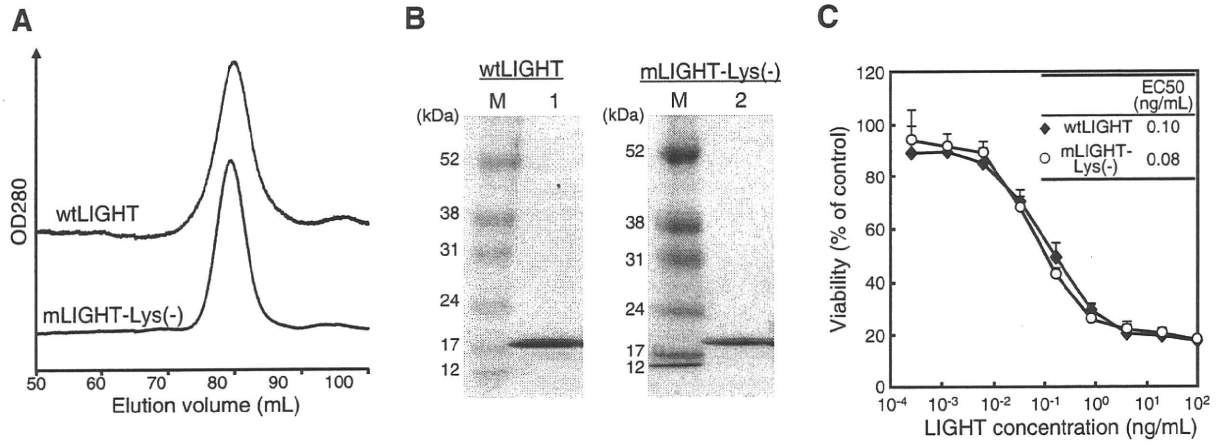

Fig. 2. Properties of recombinant mLIGHT-Lys(−), a lysine-deficient LIGHT mutant. (A) Gel-filtration analysis of purified wtLIGHT and mLIGHT-Lys(−). wtLIGHT or mLIGHT-Lys(−) was loaded onto size-exclusion column and eluted at 1.0 mL/min. (B) SDS–PAGE analysis of mLIGHT-Lys(−). Purified wtLIGHT and mLIGHT-Lys(−) were applied to a 4–20% gradient polyacrylamide gel and stained with CBB. Lane M, molecular weight standards; lane 1, wtLIGHT; lane 2, mLIGHT-Lys(−). (C) *In vitro* bioactivity of mLIGHT-Lys(−). HT29.14S cells were incubated with serial dilutions of wtLIGHT or mLIGHT-Lys(−). After 72 h incubation, cell viability was assessed with a methylene blue assay. The EC_{50} is the concentration of LIGHT required to inhibit cell viability by 50%. The data represent means ± SD ($n = 4$).

the SPR method (Table 2). The K_D, the index of associative strength, of mLIGHT-Lys(−) for LTβR and HVEM were almost the same as those of wtLIGHT, indicating that the affinity of mLIGHT-Lys(−) for LTβR and HVEM is similar to that of wtLIGHT. In contrast, the K_D of mLIGHT-Lys(−) for DcR3 was about 2-fold higher than that of wtLIGHT, indicating a loss of binding capacity for DcR3. Furthermore, detailed analysis of the kinetics indicated that the reduction in affinity of mLIGHT-Lys(−) for DcR3 was due to a higher dissociation rate constant (k_{off}) than wtLIGHT. These data suggest that mLIGHT-Lys(−) retains the same bioactivity as wtLIGHT but is more selective in binding to LTβR and HVEM.

DcR3 is overexpressed in various tumors and act as an inhibitory receptor for LIGHT [6,10,11]. Therefore, the capacity to evade DcR3 would be a great advantage for the use of LIGHT in cancer therapy. To investigate whether mLIGHT-Lys(−) is less susceptible to the inhibitory effects of DcR3, we examined the bioactivity of mLIGHT-Lys(−) in the presence of DcR3 (Fig. 3). DcR3 blocked wtLIGHT-induced cell death in a dose-dependent manner, with a 50% inhibitory concentration (IC_{50}) of 49 ng/mL, whereas the IC_{50} of DcR3 against mLIGHT-Lys(−) was 306 ng/mL (Fig. 3). These data collectively indicate that mLIGHT-Lys(−) was 6-fold more resistant to the neutralization effect of DcR3 than wtLIGHT, while retaining most of the bioactivity of wtLIGHT. From these data, we consider that mLIGHT-Lys(−) might be a superior candidate for cancer therapy. Although the structure of LIGHT has not been well defined, our data clearly showed the importance of lysine residues of LIGHT in binding to DcR3. These results would be informative for the creation of functional LIGHT mutants with receptor selectivity, high therapeutic efficiency and so on.

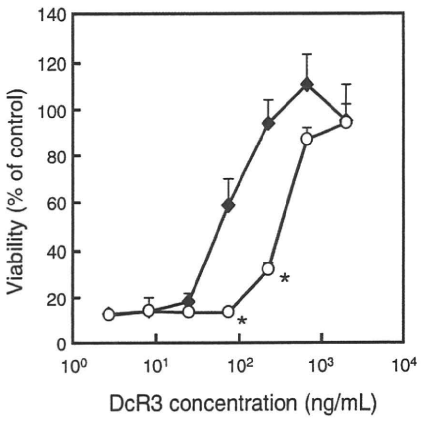

Fig. 3. Evaluation of the DcR3 interactions of mLIGHT-Lys(−). HT29.14S cells were incubated with each LIGHT (10 ng/mL) in the presence of the indicated concentrations of DcR3 for 72 h. Cell viability was determined with the methylene blue assay. The IC_{50} is the concentration of DcR3 required to inhibit the cytotoxicity of LIGHT by 50%. The data represent means ± SD ($n = 4$; $^*P < 0.05$ versus value for wtLIGHT, *t*-test.).

3.3. Site-specific PEGylation of mLIGHT-Lys(−)

To confirm that mLIGHT-Lys(−) is PEGylated specifically at NH_2-terminus, wtLIGHT and mLIGHT-Lys(−) were reacted with

Table 2
Binding properties of LIGHTs to its receptors. Binding affinities to LTβR, HVEM, or DcR3 were analyzed using BIAcore. Each kinetic parameter was calculated from the respective sensorgram using BIAevaluation 4.1 software.

	LTβR	HVEM			DcR3	
	K_D[a] (nM)	K_D[a] (nM)	k_{on}[b] (10^5/Ms)	k_{off}[c] (10^{-4}/s)	K_D[a] (nM)	Affinity (% versus wtLIGHT)
wtLIGHT	1.3	1.5	3.3	2.0	0.6	100
mLIGHT-Lys(−)	1.1	1.7	4.7	5.3	1.1	54.5
PEG-mLIGHT-Lys(−)	1.1	1.5	2.9	4.7	1.6	37.5

[a] K_D is the equilibrium dissociation constant.
[b] k_{on} is the association kinetic constant.
[c] k_{off} is the dissociation kinetic constant.

125-fold molar excess of activated PEG5K relative to the respective total primary amine groups of wtLIGHT or mLIGHT-Lys(−), respectively. PEGylated LIGHT was detected by SDS–PAGE followed by CBB staining. PEGylation of wtLIGHT resulted in multiple PEGylated bands (Fig. 4A). In contrast, the PEGylation of mLIGHT-Lys(−) led to only a single PEGylated band. These observations indicate that PEG molecules were introduced randomly at multiple positions in wtLIGHT, whereas a single PEG molecule was attached selectively to the NH_2-terminus of mLIGHT-Lys(−). We speculate that the bands under the non-PEGylated LIGHTs (Fig. 4A, lanes 1 and 3) might be degraded LIGHT.

To collect LIGHTs conjugated with one PEG molecule, wtLIGHT and mLIGHT-Lys(−) were reacted with 3- and 25-fold molar excesses, respectively, of activated PEG5K relative to the number of total primary amine groups of each type of LIGHT. We separated reacted LIGHTs by gel-filtration HPLC (Fig. 4B) and pooled peak 2 and peak 5 as LIGHTs with one PEG molecule. We then analyzed the collected proteins by SDS–PAGE, and found a single band of 27 kDa for both wtLIGHT and mLIGHT-Lys(−) (Fig. 4C). We believe that peaks 1 and 4 represent non-PEGylated LIGHT forms, and peaks 3 and 6 reflect LIGHTs conjugated with two or more PEG molecules. Thus, we obtained purified randomly PEGylated wtLIGHT and site-specific PEGylated mLIGHT-Lys(−). Then we examined their bioactivity using HT29.14S cells (Fig. 4D). PEGylated wtLIGHT and PEGylated mLIGHT-Lys(−) had activity equal to that of non-PEGylated wtLIGHT and mLIGHT-Lys(−), respectively. Next, to investigate the capacity of PEGylated mLIGHT-Lys(−) to avoid the inhibitory effects of DcR3, we examined the bioactivity of PEGylated mLIGHT-Lys(−) in the presence of DcR3 (Fig. 4E). We found that PEGylated mLIGHT-Lys(−) retained its DcR3 evading effect as mLIGHT-Lys(−). Furthermore, using the SPR method, we confirmed that the binding kinetics of PEGylated mLIGHT-Lys(−) for LTβR, HVEM, and DcR3 were almost same as those of non-PEGylated mLIGHT-Lys(−) (Table 2). These results collectively indicate that PEGylated mLIGHT-Lys(−) has excellent molecular uniformity and retains high activity even in the presence of DcR3.

In general, conventional PEGylation of cytokines causes a loss of bioactivity due to random introduction of PEG at lysine residues. For instance, PEGylated IFN-α has been clinically used for the treatment of hepatitis C. The PEGylated IFN-α, which is a mixture of various positional isomers, has about 10% of its bioactivity compared to unmodified IFN-α [19]. Thus, clinical application of PEGylated proteins has been limited in most cases, except for some bioactive proteins, such as IFN-α. In this study, PEGylated wtLIGHT

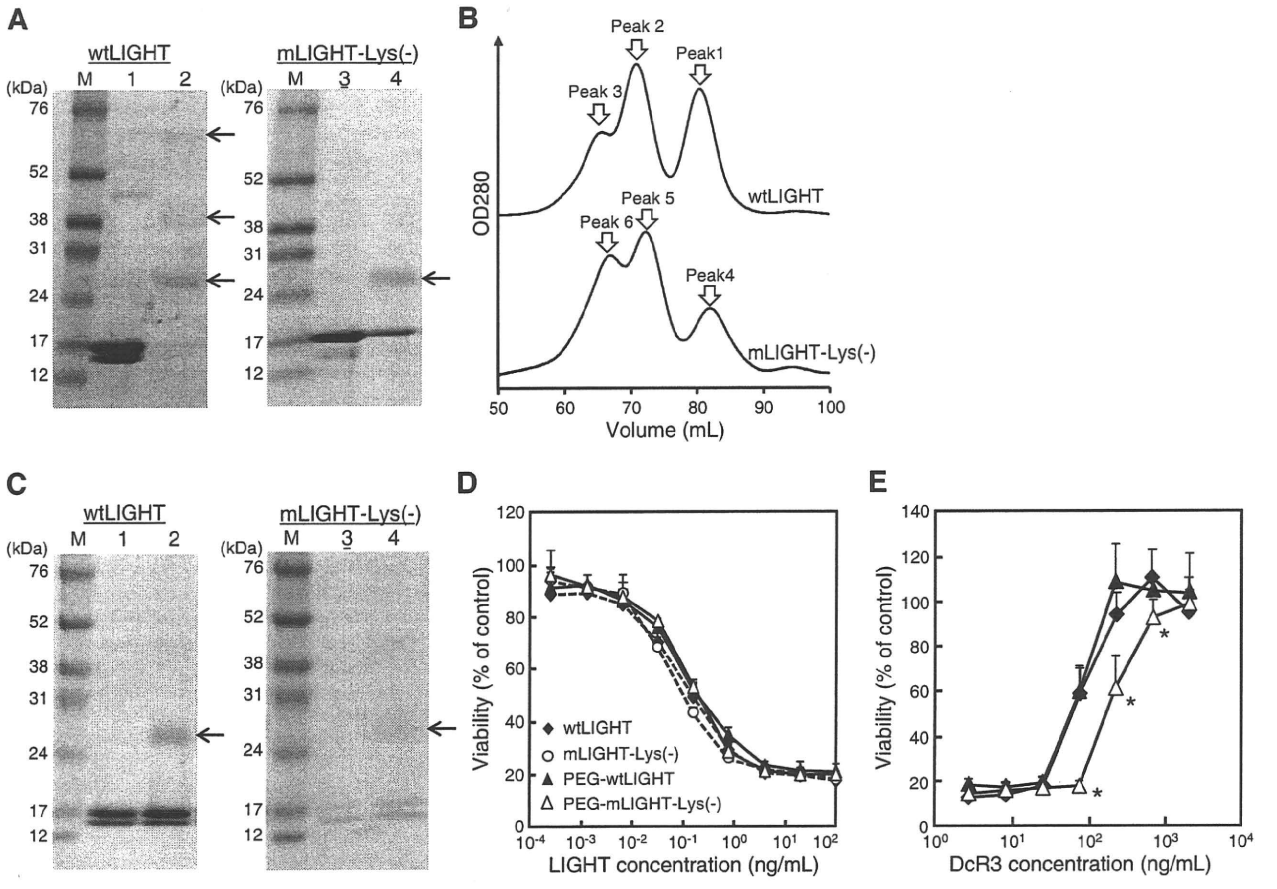

Fig. 4. Properties of site-specific PEGylated mLIGHT-Lys(−). (A) SDS–PAGE analysis of PEGylated LIGHTs. wtLIGHT and mLIGHT-Lys(−) was reacted with PEG5K. SDS–PAGE analysis of PEGylated LIGHTs was conducted, and stained with CBB. Lane M, molecular weight standards; lane 1, wtLIGHT; lane 2, PEG-wtLIGHT; lane 3, mLIGHT-Lys(−); lane 4, PEG-mLIGHT-Lys(−). Arrows indicate PEGylated LIGHT. (B,C) The collection of PEGylated LIGHTs. (B) Gel-filtration analysis of PEGylated LIGHTs. wtLIGHT (upper) and mLIGHT-Lys(−) (lower) reacted with PEG5K were loaded onto size-exclusion columns and eluted at 1.0 mL/min. (C) SDS–PAGE analysis of PEGylated LIGHTs was conducted, and stained with CBB. Lane M, molecular weight standards; lane 1, wtLIGHT; lane 2, PEG-wtLIGHT; lane 3, mLIGHT-Lys(−); lane 4, PEG-mLIGHT-Lys(−). Arrows indicate PEGylated LIGHT. (D) *In vitro* bioactivity of PEGylated LIGHTs. HT29.14S cells were incubated with various concentrations of each LIGHT for 72 h. Cell viability was determined with the methylene blue assay. (E) The ability of PEG-mLIGHT-Lys(−) to evade DcR3. HT29.14S cells were incubated with each LIGHT (10 ng/mL) in the presence of various concentrations of DcR3 for 72 h. Cell viability was determined with the methylene blue assay. The data represent means ± SD ($n = 4$; $^*P < 0.05$ versus the value for wtLIGHT, *t*-test.).

had bioactivity similar to that of wtLIGHT. These results indicate that the lysine residues of LIGHT are not associated with its binding to LTβR and HVEM. However, PEGylated wtLIGHT was likely a mixture of various positional isomers, whereas PEGylated mLIGHT-Lys(−) had PEG only at the NH_2-terminus. The uniform molecular structure of PEGylated mLIGHT-Lys(−) showed no loss of bioactivity, but had lower affinity for DcR3. These features suggest that PEGylated mLIGHT-Lys(−) might be a superior candidate for cancer therapy. On the other hand, there is a possibility that mLIGHT-Lys(−) binds to any other receptors different from that of wtLIGHT because of the conformational change. Such unexpected binding, called off-target effect, might induce severe side effect [24]. We are now examining the safety and efficacy of PEGylated mLIGHT-Lys(−) *in vivo*.

In this study, mLIGHT-Lys(−) was conjugated to linear PEG5K, which is widely used for PEGylation of proteins, as a first approach. However, the molecular weight and the shape of PEG strongly influence the *in vivo* stability of the modified protein [25]. For instance, the *in vivo* stability increases with increasing molecular weight of PEG, whereas its *in vitro* bioactivity tends to decrease because of the steric hindrance [26]. Our group has previously reported that the optimization of the molecular weight or the shape of PEG strongly improves the antitumor activity [15]. Therefore, for maximizing the effectiveness of PEGylation, it will be important to select the optimal molecular weight or type of PEG, balancing favorable effects, side effects, and dose schedule. We believe that such optimization of PEG molecule will lead to more improvements in the usefulness of mLIGHT-Lys(−).

4. Conclusion

Here, we created a fully bioactive lysine-deficient LIGHT mutant by using a phage display technique and successfully obtained a site-specific PEGylated LIGHT mutant with molecular uniformity and retained bioactivity. Furthermore, we confirmed that mLIGHT-Lys(−) has lower affinity for DcR3. A better understanding of the correlation between structure, kinetic behavior, and activity will likely accelerate drug discovery because of increased awareness of the properties of therapeutic proteins. We suggest that mLIGHT-Lys(−) might be a powerful tool for cancer therapy, and we believe that our data offer valuable information for the construction of even more functional LIGHT mutants.

Acknowledgments

The authors declare no conflict of interests. This study was supported in part by grants from the Ministry of Health, Labor, and Welfare of Japan; by a Research on Health Sciences Focusing on Drug Innovation grant from the Japan Health Sciences Foundation; and by the Takeda Science Foundation.

References

[1] J.A. Harrop, P.C. McDonnell, M. Brigham-Burke, et al., Herpesvirus entry mediator ligand (HVEM-L), a novel ligand for HVEM/TR2, stimulates proliferation of T cells and inhibits HT29 cell growth, J. Biol. Chem. 273 (1998) 27548–27556.
[2] M. Murphy, B.N. Walter, L. Pike-Nobile, et al., Expression of the lymphotoxin beta receptor on follicular stromal cells in human lymphoid tissues, Cell Death Differ. 5 (1998) 497–505.
[3] P. Stopfer, D.N. Mannel, T. Hehlgans, Lymphotoxin-beta receptor activation by activated T cells induces cytokine release from mouse bone marrow-derived mast cells, J. Immunol. 172 (2004) 7459–7465.
[4] P. Yu, Y. Lee, W. Liu, et al., Priming of naive T cells inside tumors leads to eradication of established tumors, Nat. Immunol. 5 (2004) 141–149.
[5] K. Tamada, K. Shimozaki, A.I. Chapoval, et al., LIGHT, a TNF-like molecule, costimulates T cell proliferation and is required for dendritic cell-mediated allogeneic T cell response, J. Immunol. 164 (2000) 4105–4110.
[6] Y. Wu, B. Han, H. Sheng, et al., Clinical significance of detecting elevated serum DcR3/TR6/M68 in malignant tumor patients, Int. J. Cancer 105 (2003) 724–732.
[7] R.M. Pitti, S.A. Marsters, D.A. Lawrence, et al., Genomic amplification of a decoy receptor for Fas ligand in lung and colon cancer, Nature 396 (1998) 699–703.
[8] C. Bai, B. Connolly, M.L. Metzker, et al., Overexpression of M68/DcR3 in human gastrointestinal tract tumors independent of gene amplification and its location in a four-gene cluster, Proc. Natl. Acad. Sci. USA 97 (2000) 1230–1235.
[9] S. Macher-Goeppinger, S. Aulmann, N. Wagener, et al., Decoy receptor 3 is a prognostic factor in renal cell cancer, Neoplasia 10 (2008) 1049–1056.
[10] R.M. Gill, J.S. Hunt, Soluble receptor (DcR3) and cellular inhibitor of apoptosis-2 (cIAP-2) protect human cytotrophoblast cells against LIGHT-mediated apoptosis, Am. J. Pathol. 165 (2004) 309–317.
[11] S. Hayashi, Y. Miura, T. Nishiyama, et al., Decoy receptor 3 expressed in rheumatoid synovial fibroblasts protects the cells against Fas-induced apoptosis, Arthritis Rheum. 56 (2007) 1067–1075.
[12] T. Morishige, Y. Yoshioka, H. Inakura, et al., LIGHT protein suppresses tumor growth by augmentation of immune response, Immunol. Lett. 127 (2009) 33–38.
[13] Y. Yoshioka, Y. Tsutsumi, S. Nakagawa, et al., Recent progress on tumor missile therapy and tumor vascular targeting therapy as a new approach, Curr. Vasc. Pharmacol. 2 (2004) 259–270.
[14] Y. Mukai, Y. Yoshioka, Y. Tsutsumi, Phage display and PEGylation of therapeutic proteins, Comb. Chem. High Throughput Screen. 8 (2005) 145–152.
[15] Y. Yoshioka, Y. Tsutsumi, S. Ikemizu, et al., Optimal site-specific PEGylation of mutant TNF-alpha improves its antitumor potency, Biochem. Biophys. Res. Commun. 315 (2004) 808–814.
[16] H. Shibata, Y. Yoshioka, S. Ikemizu, et al., Functionalization of tumor necrosis factor-alpha using phage display technique and PEGylation improves its antitumor therapeutic window, Clin. Cancer Res. 10 (2004) 8293–8300.
[17] H. Shibata, Y. Yoshioka, A. Ohkawa, et al., Creation and X-ray structure analysis of the tumor necrosis factor receptor-1-selective mutant of a tumor necrosis factor-alpha antagonist, J. Biol. Chem. 283 (2008) 998–1007.
[18] H. Shibata, Y. Yoshioka, Y. Abe, et al., The treatment of established murine collagen-induced arthritis with a TNFR1-selective antagonistic mutant TNF, Biomaterials 30 (2009) 6638–6647.
[19] Y.S. Wang, S. Youngster, M. Grace, et al., Structural and biological characterization of pegylated recombinant interferon alpha-2b and its therapeutic implications, Adv. Drug Deliv. Rev. 54 (2002) 547–570.
[20] Y. Yamamoto, Y. Tsutsumi, Y. Yoshioka, et al., Site-specific PEGylation of a lysine-deficient TNF-alpha with full bioactivity, Nat. Biotechnol. 21 (2003) 546–552.
[21] I.A. Rooney, K.D. Butrovich, A.A. Glass, et al., The lymphotoxin-beta receptor is necessary and sufficient for LIGHT-mediated apoptosis of tumor cells, J. Biol. Chem. 275 (2000) 14307–14315.
[22] T. Morishige, Y. Yoshioka, H. Inakura, et al., Creation of a LIGHT mutant with the capacity to evade the decoy receptor for cancer therapy, Biomaterials (2010) (Epub ahead of print).
[23] Y. Yoshioka, H. Watanabe, T. Morishige, et al., Creation of lysine-deficient mutant lymphotoxin-alpha with receptor selectivity by using a phage display system, Biomaterials 31 (2009) 1935–1943.
[24] C.P. Miller, C.A. Blau, Using gene transfer to circumvent off-target effects, Gene Ther. 15 (2008) 759–764.
[25] B. Treetharnmathurot, C. Ovartlarnporn, J. Wungsintaweekul, et al., Effect of PEG molecular weight and linking chemistry on the biological activity and thermal stability of PEGylated trypsin, Int. J. Pharm. 357 (2008) 252–259.
[26] P. Caliceti, F.M. Veronese, Pharmacokinetic and biodistribution properties of poly(ethylene glycol)-protein conjugates, Adv. Drug Deliv. Rev. 55 (2003) 1261–1277.